	Form Approved OMB NO. 0704-0188

1. AGENCY USE ONLY (Leave Blank)	2. REPORT DATE	3. REPORT TYPE AND DATES COVERED
	01 May 07	Final Report 01/Oct/04 - 30/Sep/06

4. TITLE AND SUBTITLE	5. FUNDING NUMBERS
Lotus LADM Based Self-Decontaminating Surfaces	W911NF-04-C-0081
6. AUTHOR(S) John L. Lombardi, Ph.D. Prof. S. Michielsen, Prof. R.E. Connors, & Prof. Churchward	
7. PERFORMING ORGANIZATION NAME(S) AND ADDRESS(ES) John L. Lombardi, Ph.D. Ventana Research Company 831 N. Camino Miramonte Tucson, AZ 85716	8. PERFORMING ORGANIZATION REPORT NUMBER Proposal # 4439- CH-DRP
9. SPONSORING / MONITORING AGENCY NAME(S) AND ADDRESS(ES) U. S. Army Research Office P.O. Box 12211 Research Triangle Park, NC 27709-2211	10. SPONSORING / MONITORING AGENCY REPORT NUMBER 44349.1-CH-DRP

11. SUPPLEMENTARY NOTES

The views, opinions and/or findings contained in this report are those of the author(s) and should not be construed as an official Department of the Army position, policy or decision, unless so designated by other documentation.

12 a. DISTRIBUTION / AVAILABILITY STATEMENT	12 b. DISTRIBUTION CODE
Approved for public release; distribution unlimited.	

13. ABSTRACT (Maximum 200 words)

Recent events have lead to new concerns about biowarfare, bioterrorism, chemical warfare and chemical terrorism. Because of the potential range of biological and chemical agents that could be used, a non-specific decontamination system is desirable. Of particular interest are materials whose surfaces have been modified to be self-decontaminating and self-regenerating. Other beneficial attributes are that the surfaces be self-cleaning and very light weight. We have developed superhydrophobic coating materials having water droplet wetting contact angles up to 178•. We have also developed Light Activated Decontamination Materials, LADM, that produce singlet oxygen. In addition a series of novel sporicidal compounds were synthesized having thiolate functionality. We have characterized both the LADM photophysical properties as well as the interaction between thiolate based sporicides and singlet oxygen. The LADM surface modification can be made with a wide range of colors to allow color matching to nearly any color desired by the military. Our approach simultaneously addresses all three thrust areas, surface modification, self-cleaning, antimicrobial and sporicidal activity. Our photo-active agents absorb visible light and transfer the energy to oxygen in the air to generate singlet oxygen, which has been shown to destroy chemical and biological agents.

14. SUBJECT TERMS	15. NUMBER OF PAGES
Self-decontaminating, LADM, Photosensitizer, Superhydrophobic, Flocking	
	16. PRICE CODE

17. SECURITY CLASSIFICATION OR REPORT	18. SECURITY CLASSIFICATION ON THIS PAGE	19. SECURITY CLASSIFICATION OF ABSTRACT	20. LIMITATION OF ABSTRACT
UNCLASSIFIED	**UNCLASSIFIED**	**UNCLASSIFIED**	**UL**

NSN 7540-01-280-5500

Standard Form 298 (Rev.2-89)
Prescribed by ANSI Std. 239-18
298-102

LOTUS-LADM BASED SELF DECONTAMINATING SURACES
Contract # W911NF-04-C-0081
John L. Lombardi, Ventana Research Corporation (Tucson, AZ)
Stephen Michielsen, North Carolina State University (Raleigh, NC)
Robert Connors, Worcester Polytechnic Institute (Worcester, MA)
Gordon Churchward, Emory University (Atlanta, GA)

Executive Summary

Recent events have lead to new concerns about biowarfare, bioterrorism, chemical warfare and chemical terrorism. Because of the potential range of biological and chemical agents that could be used, a non-specific decontamination system is desirable. Of particular interest are materials whose surfaces have been modified to be self-decontaminating and self-regenerating. Other beneficial attributes are that the surfaces be self-cleaning and very light weight. We have developed superhydrophobic coating materials having water droplet wetting contact angles up to 178°. We have also developed Light Activated Decontamination Materials, LADM, that produce singlet oxygen. In addition a series of novel sporicidal compounds were synthesized having thiolate functionality. Professor Connors has characterized both the LADM photophysical properties as well as the interaction between thiolate based sporicides and singlet oxygen. The LADM surface modification can be made with a wide range of colors to allow color matching to nearly any color desired by the military. These materials were shipped to Prof. Gordon Churchward, Emory University, for analysis of their antimicrobial and sporicidal activity.

Our approach simultaneously addresses all three thrust areas, surface modification, self-cleaning, and sporicide. To form our LADM coatings, a 10 nm thick scaffold polymer was bonded to the surface of fibers. Then photo-active agents were grafted to this scaffold polymer. This increased the available photo-active agents >1000 fold, while adding less than 0.1 wt % to the fibers. These photo-active agents absorb visible light and transfer the energy to oxygen in the air to generate singlet oxygen, which has been shown to destroy chemical and biological agents. From the mode of action, singlet oxygen was also expected to destroy spores.

Self-cleaning surfaces rely on the Lotus effect in which water is suspended upon a hydrophobic surface with air gaps between different segments of the hydrophobic material. The droplet is supported on the raised portions with air gaps below large portions of the droplet. To render the surface superhydrophobic, or self-cleaning, we bonded short fibers to the surface through flocking. By controlling the flocking process, we could control the fiber height and spacing. These two factors have been shown to be important to generating the Lotus effect. This was not be sufficient to render the surface superhydrophobic. However, by modifying the surface further with fluorochemical or long chain alkanes, we were able to convert the surface from hydrophobic to superhydrophobic.

Technical Section

This report describes our efforts to develop superhydrophobic soft materials and soft materials that produce singlet oxygen for decontamination. We have developed a self-decontaminating surface based on the synthesis of $^1\Delta_g$ oxygen (singlet oxygen) from photoactive organic dyes. The process to make this material is compatible with the process to make the surface superhydrophobic. We first describe our superhydrophobic materials.

SELF-CLEANING SURFACES

Superhydrophobic surfaces are defined as surfaces upon which water has an apparent contact angle of greater than 150°. A common description of these surfaces is that they are self-cleaning since water beads up and rolls off the surface carrying surface debris with it, much in the same way that water beads up and flows off of the Lotus leaf. The surface is described as exhibiting the Lotus effect. Otten and Herminghaus [1] have noted that the Lotus effect occurs by two distinctly different mechanisms. (1) The first method relies on a rough hydrophobic surface where the size scale of the roughness is much smaller than the size of a water droplet, 50-500 μm. The Indian Cress (*Tropaeloum majus L.)* exhibits this type of Lotus effect. In this case there are at least two size scales, that of the individual plant cells (~20 μm), the size of the wax crystals b(~1μm), and the distance between wax crystals (~5 μm). This combination has been shown to be superhydrophobic. (2) The other mechanism for providing superhydrophobicity is exhibited by the Lady's Mantle (*Alchemilla vulgaris L.)* In this case, the surface is covered with *hydrophilic* hairs, but the leaf is still superhydrophobic. This has been attributed to the energy required to bend the hairs. When a water droplet is placed on the hairs, they coalesce by bending. This costs energy, which is sufficient to lift the droplet from the hydrophobic surface onto the hydrophilic fibers, resulting in a superhydrophobic surface. Manufacturing similar structures is a daunting task.

EXPERIMENTAL

Materials

Nylon 6,6 film (Mn:12 kD, Dupont), polyester fabric (93g/m^2), acrylic adhesive (C. L. Hauthaway & Sons Co.), and an electrostatic flock applicator (CP-70, Cellusuede Products. Inc.) were used for the smooth surfaces or the design of rough surfaces. Various nylon 6,6 rod-shaped short fibers (flock fibers, Cellusuede) were applied to polyester fabric, Poly(acrylic acid) (PAA, M_w: 450kD, Aldrich), 4-(4,6-dimethoxy-1,3,5-triazin-2yl)-4-methylmorpholinium chloride (DMTMM, Fluka), sodium thiocyanate (NaSCN, Fisher), Methanol (Aldrich), and 1H, 1H-perfluorooctylamine ($C_8H_4F_{15}N$, Synquest), laurylamine, Polyisobutylene-alt-maleic anhydride (PIBMA, Isobam M_w: 60kD, Kuraray Co., Ltd.), Dytek EP 1,3-pentanediamine (INVISTA), KOH (reagent grade), chloroaluminum phthalocyanine (AlPc Sanyo Color Works, Ltd.), chlorosulfonic acid (reagent grade – duPont), phosphorus oxychloride (reagent grade, Aldrich) were used without further purification.

Preparation of Rough Surfaced Nylon Composite

The electrostatic flock applicator produces a 30 to 70kV potential to drive the rod-shaped nylon flock fibers from the container of the applicator to the polyester substrate fabric resting on a metal grounding plate (Figure 1).

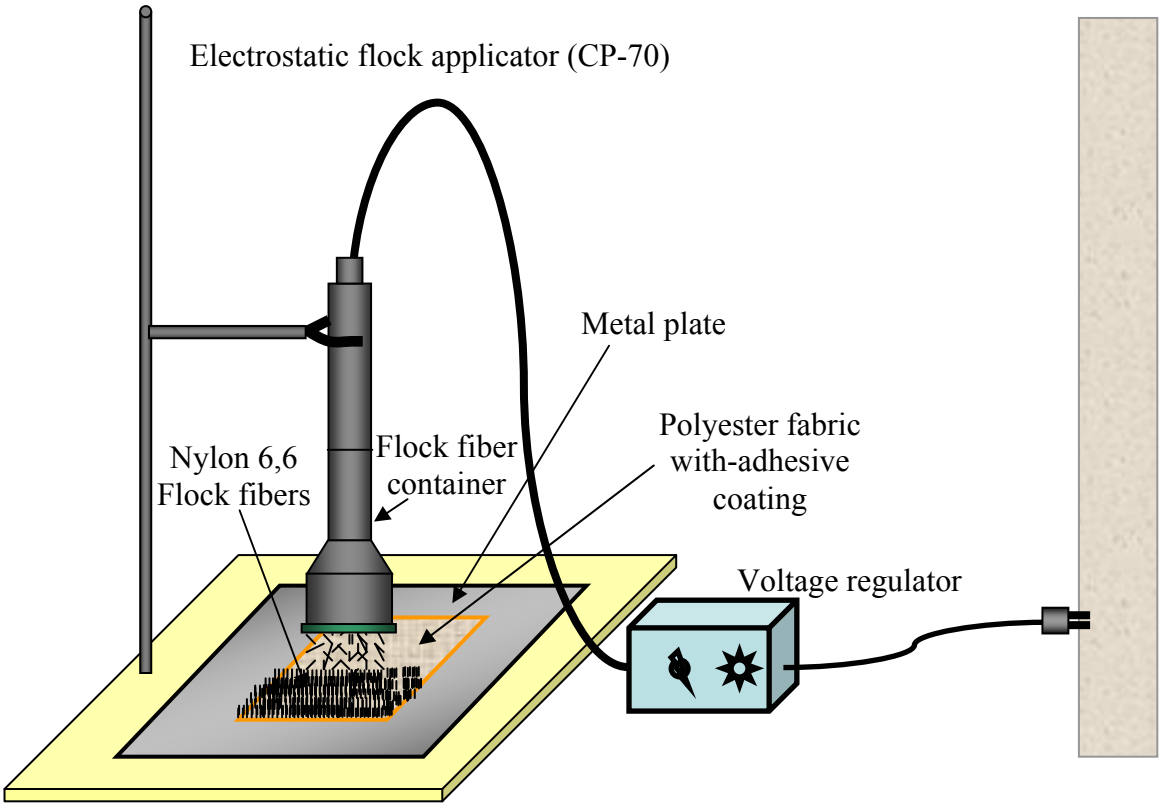

Figure 1. Application of nylon flock fibers to polyester substrate.

A 10x10cm^2 polyester fabric was coated with 0.3g of acrylic adhesive by screen-printing. The nylon flock fibers were shot from the applicator for five seconds vertically down into the adhesive that had previously been applied to a polyester substrate. The flock fibers oriented in the flow direction to reduce their air resistance through this process, and those fibers were perpendicularly aligned to the polyester substrate. The fabric was dried at 120℃ for 10 minutes and cured at 149°C for 5 minutes after pre-cleaning to remove unattached flock.

Grafting of PAA on Nylon 6,6 Film Surface

0.1g PAA was dissolved in 500ml distilled water at 20℃. Then 0.62g nylon 6,6 film (10x10cm^2) was immersed in the PAA solution for 24 hours, rinsed in distilled water with stirring for 8 hours (repeated three times with fresh water), wiped with a Kimwipe^{TM} and air dried. Next, 0.15g DMTMM was dissolved in distilled water with vigorous stirring at 20℃. A PAA adsorbed film was immersed in the DMTMM solution for the graft of PAA to the nylon surface. The reaction was allowed to proceed for 2 hours. PAA grafted film was rinsed in distilled water for 8 hours (repeated three times with fresh solvent), wiped with a Kimwipe^{TM}, and air dried.

To remove non grafted PAA from the nylon film, the film was rinsed in a 1M aqueous sodium thiocyanate (NaSCN) solution with stirring (repeated twice with fresh solution), rinsed in distilled water for 8 hours (repeated three times with fresh solution), and heated in water for 3 hours at 65℃. Then, the film was wiped with a Kimwipe^{TM} and air dried.

Grafting of 1H, 1H-Perfluorooctylamine on PAA Grafted Nylon 6,6 Film Surface

0.1g 1H, 1H-perfluorooctylamine was dissolved in 10ml methanol at 20℃. Then 0.31g PAA grafted nylon 6,6 film (5x10 cm^2) was immersed in the fluoroamine solution for 24 hours with stirring. Then, 0.07g DMTMM was dissolved in methanol with vigorous stirring at 20℃. A fluoroamine adsorbed PAA grafted nylon film was immersed in the DMTMM solution for the graft of fluorochemical to the PAA on nylon 6,6 surface. The reaction proceeded for 2 hours. The fluoroamine grafted PAA grafted nylon film was rinsed in methanol for 8 hours (repeated twice with fresh solvent), rinsed in distilled water for 8 hours (repeated twice with fresh solvent), wiped with a Kimwipte^{TM}, and air dried.

Grafting of PAA on Rough Nylon 6,6 Surface

1g PAA was dissolved in 1L distilled water at 20℃. Then a 11g PAA grafted nylon 6,6 rough surface composite (10x10cm^2) consisting of 1g polyester substrate was immersed in the PAA solution for 24 hours, rinsed in distilled water with stirring for 8 hours (repeated six times with fresh water), wiped with a Kimwipe^{TM} and air dried. Next, 1.5g DMTMM was dissolved in distilled water with vigorous stirring at 20℃. A PAA adsorbed nylon composite was immersed in the DMTMM solution for the graft of PAA to the nylon surface. The reaction proceeded for 2 hours. The PAA grafted nylon composite was rinsed in distilled water for 8 hours (repeated six times with fresh solvent), wiped with a Kimwipe^{TM}, and air dried. To remove excess PAA that had not grafted to the nylon composite, the composite was rinsed in a 1M aqueous sodium thiocyanate (NaSCN) solution with vigorous stirring (repeated twice with fresh solution), rinsed in distilled water for 8 hours (repeated six times with fresh solution), and heated in water for 3 hours at 65℃. Then, the composite was wiped with a Kimwipe^{TM} using a combing action and air dried.

Grafting of 1H, 1H-Perfluorooctylamine on PAA Grafted Rough Nylon 6,6 Surface

1g 1H, 1H-perfluorooctylamine was dissolved in 100ml methanol at 20℃. Then 2.8g PAA grafted nylon 6,6 rough surface composite (5x5cm^2) was immersed in the fluoroamine solution for 24 hours with stirring. Next, 0.7g DMTMM was dissolved in methanol with vigorous stirring at 20℃. A fluoroamine adsorbed PAA grafted nylon composite was immersed in the DMTMM solution for the graft of fluoroamine to the PAA on nylon 6,6 surface. The reaction proceeded for 2 hours. The fluoroamine grafted PAA grafted nylon composite was rinsed in methanol for 8 hours (repeated four times with fresh solvent), rinsed in distilled water for 8 hours (repeated twice with fresh solvent), combed with a Kimwipte^{TM}, and air dried.

Scanning Electron Microscopy

The rough surface nylon composite was examined with a scanning electron microscope (SEM), Hitachi S-3200N, operated at 10kV and magnifications from 50x to 2000x. For the analysis of SEM pictures, an image program (Image J 1.34s, National Institute of Health) was used.

Contact Angle Measurements

The contact angle on the prepared surfaces was measured with sessile water drops using a lab-designed goniometer at 20℃. The contact angle images were obtained using an optical contact angle measurer (VCA Optima, AST Products Inc.). The volume of the applied droplets of

distilled water was 10μL. Mean values were calculated from at least four individual measurements each on a new spot.

RESULTS AND DISCUSSION

To form a superhydrophobic surface, the surface must have a low surface tension *and* be rough. We used a two stage procedure to create a superhydrophobic fabric. First, we modified nylon film to generate a low surface tension surface. Then we made a rough nylon surface via the flocking process and modified the nylon flock fibers to give them a low surface tension using the same procedure as for the nylon film.

According to equation (1), a water droplet (γ_L^d = 21.8, γ_L^p = 1.4, and γ_L^H = 49.6 dyne/cm) placed upon a clean, smooth nylon surface (γ_S^d = 40.8 and γ_S^H = 6.2 dyne/cm) should have a contact angle θ_e = 72º [2,3]. The values of the water contact angles measured on clean nylon film in this study are 65º < θ_e < 73º, in good agreement with the predicted value.

$$\gamma_L(1+\cos\theta_e) = 2\left(\sqrt{\gamma_S^d \cdot \gamma_L^d} + \sqrt{\gamma_S^p \cdot \gamma_L^p} + \sqrt{\gamma_S^H \cdot \gamma_L^H}\right) \quad (1)$$

To make the nylon film surface hydrophobic, we need to attach a low surface tension material to the nylon surface. However, nylon has very few reactive sites, so first we must modify the surface to increase the number of reactive sites. Using the procedure developed by Tobiesen and Michielsen[4] and as modified by Thompson[5] we first grafted PAA onto the film. PAA was used as a mediator between nylon 6,6 and a fluoroamine due to the high density of carboxylic acid groups along the backbone of PAA. The carboxylic acid groups of PAA are covalently grafted to the amino groups of nylon 6,6 using a triazine-based condensing reagent, DMTMM. Since PAA is more hydrophilic than nylon, the water contact angle on PAA-grafted nylon film should be less than 72º. The water contact angles measured on smooth PAA-grafted nylon film made as described in the experimental section were found to be 43º < θ_e < 50º, in agreement with the values found by Thompson[5]

Next, to make the surface hydrophobic, 1H, 1H-perfluorooctylamine was grafted onto the PAA-grafted nylon films, again using DMTMM as a condensing agent following the procedures described by Thompson. When water is placed on a clean, smooth poly(tetrafluoroethylene) (PTFE) surface (γ_S^d = 18.5 dyne/cm), θ_e = 117º [6,7]. The water contact angles measured on the fluoroamine-grafted, PAA-grafted nylon films were 93º < θ_e < 110º. These values are in agreement with those found by Thompson, but lower than expected for a fluorochemical surface. Thompson and Michielsen attributed this difference to incomplete coverage of the surface via grafting and showed that approximately 80% of the PAA is covered by fluoroamine [8]. Thus, by chemically grafting 1H, 1H-perfluorooctylamine onto PAA that has previously been grafted to a nylon surface, the surface is rendered hydrophobic. We use this procedure to make our rough surface hydrophobic, as described below.

The next step in the process of making a superhydrophobic material is to generate an appropriate rough surface. The two predominant approaches of modeling the wetting of a rough surface are the Wenzel and the Cassie-Baxter models. According to these models, a surface of a composite material can be superhydrophobic when the material consists of a rough surface having appropriate roughness, *r*, and the area fraction of the surface in contact with water, Φ_S, as shown

in equations (2) and (3), where θ_r^W is the apparent water contact angle according to the Wenzel model and θ_r^{CB} is the apparent water contact angle according to the Cassie-Baxter model.

$$\cos\theta_r^{W} = r\cos\theta_e \tag{2}$$

$$\cos\theta_r^{CB} = \Phi_S(\cos\theta_e + 1) - 1 \tag{3}$$

In this study, rod-shaped nylon flock fibers were attached on a polyester substrate. The protruding flock fibers can be thought of as pillars sticking up from the fabric surface as depicted in Figure 2.

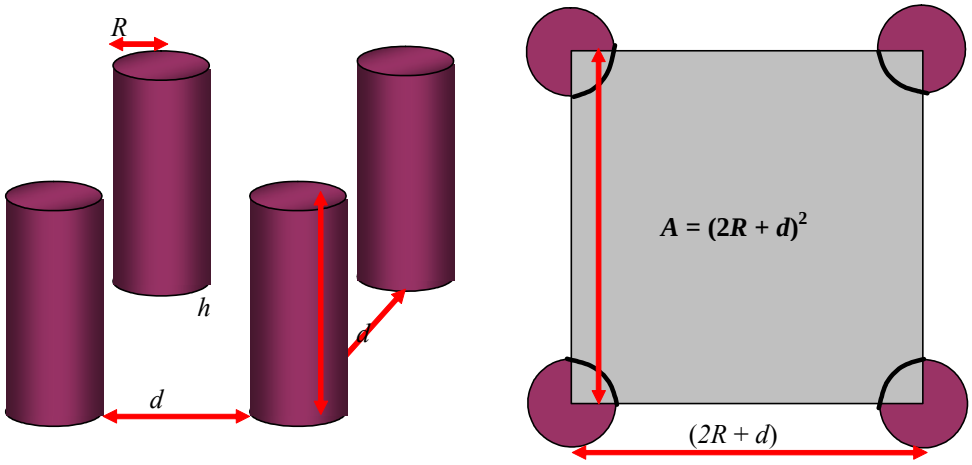

Figure 2. Side and top views of roughness pattern.

For this rough surface, r and Φ_S are defined as:

$$r = \frac{2\pi Rh}{(2R+d)^2} + 1 \tag{4}$$

$$\Phi_S = \frac{\pi R^2}{(2R+d)^2} \tag{5}$$

where R and h are the radius and height of a flock fiber, respectively; and d is the distance between two adjacent fibers. Reformulating the Wenzel and the Cassie-Baxter equations gives:

$$\cos\theta_r^{W} = \left(\frac{2\pi Rh}{(2R+d)^2} + 1\right)\cos\theta_e \tag{6}$$

$$\cos\theta_r^{CB} = \frac{\pi R^2}{(2R+d)^2}(\cos\theta_e + 1) - 1 \tag{7}$$

Figure 3 shows the regions of roughness, r, and the wetted area fraction, Φ_S, for the development of a superhydrophobic surface ($\theta_r \geq 150°$) when a rough surface is covered by fluoroamine ($\theta_e = 119°$). The graph shows that a rough surface becomes superhydrophobic when $r \geq 1.79$ and $\Phi_S \leq 26\%$.

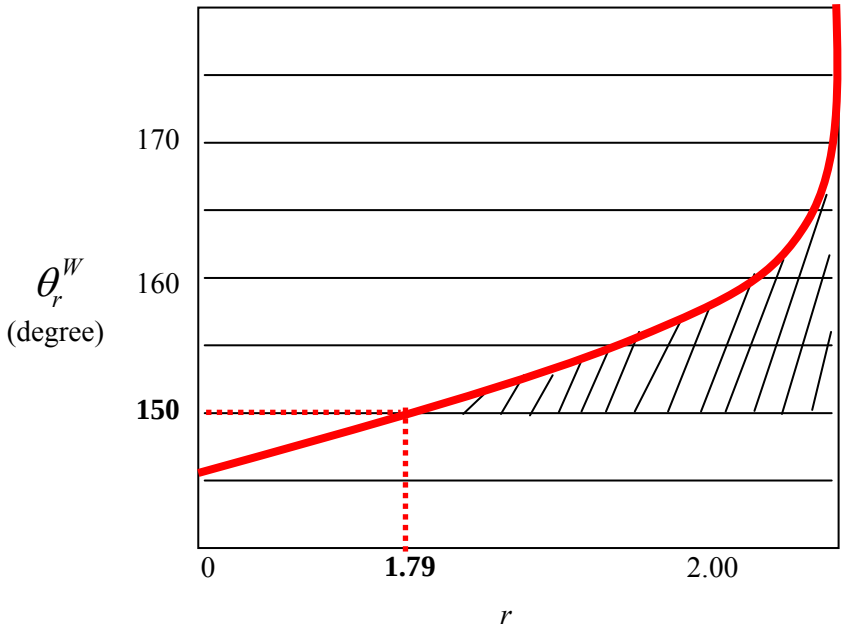

(a)

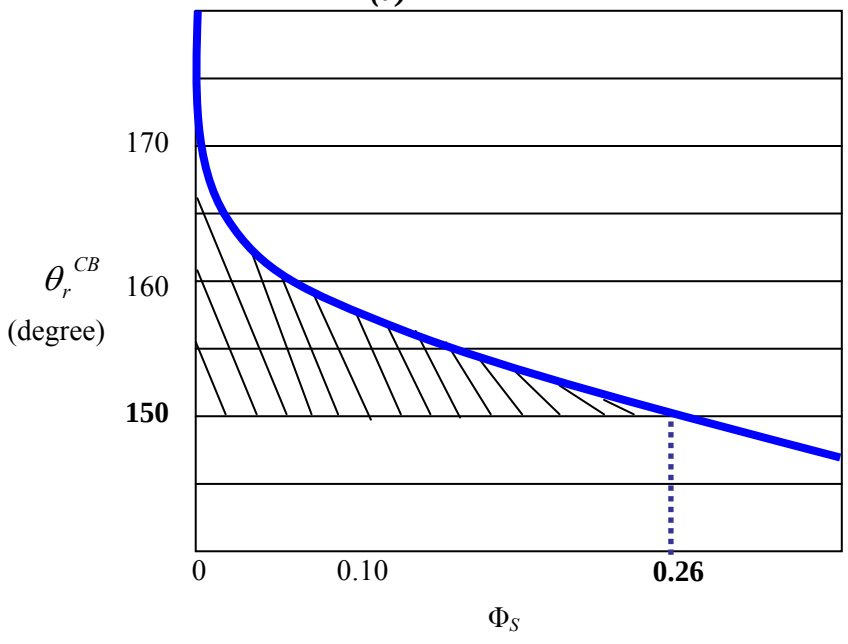

(b)

Figure 3. Plots of apparent water contact angles on a fluoroamine covered rough surface in Wenzel (a), and Cassie-Baxter (b) model; r and Φ_S are given by equations (4) and (5), respectively. Crosshatched areas indicate the superhydrophobic regions.

Four kinds of rough surfaces having different dimensions were fabricated. Table 1 describes the geometric parameters of the nylon fibers used to generate the rough surfaces. Each surface is identified as nylon flock, NF, and the height to radius ratio. For example, NF70 is made with nylon flock fibers with a height to radius ratio of 70.

Table 1. Dimensions of the nylon pillar shaped fibers

Sample	Dimensions			
	dTex*	Radius** (μm)	Height (μm)	Height / Radius
NF50	3.3	10	500	50
NF70	1.7	7	500	70
NF100	3.3	10	1000	100
NF140	1.7	7	1000	140

* Linear density: 1 dTex = 1g / 10,000m

** Calculated by linear density of each fiber and density of nylon 6,6 (1.14 g/cm^3)

If the surface of these fibers is modified to have a surface tension of 18.5 dyne/cm, equations (6) and (7) predict the surface will be superhydrophobic if the adjacent fibers have the spacings listed in Table 2.

Table 2. Designed and measured distances between two adjacent flock fibers and water contact angles after fluoroamine graft

Sample	Superhydrophobic distance range (μm)		Measured distances* (μm)	Roughness, *r* (equation 10)	Area fraction, Φ*S* (equation 11)
	Wenzel model (μm)	Cassie-Baxter model (μm)			
NF50	d < 180	d > 20	5 < d < 120	2.6 < r < 51.3	0.016 < ΦS < 0.503
NF70	d < 153	d > 10	10 < d < 120	2.2 < r < 39.2	0.009 < ΦS < 0.267
NF100	d < 263	d > 20	25 < d < 76	7.8 < r < 32.0	0.034 < ΦS < 0.155
NF140	d < 223	d > 10	10 < d < 78	6.2 < r < 77.4	0.018 < ΦS < 0.267

* Measured at twenty random spots

The maximum distance between two flock fibers on each rough surface is obtained from the Wenzel equation while the Cassie-Baxter equation gives the minimum distance between two flock fibers [9]. This table also shows the measured interfiber distances measured on adjacent fibers at 20 different locations on each sample, r (equation 6), and Φ_S (equation 7).

For example, for 14 μm diameter and 1mm long nylon pillars on the polyester substrate in an upright position, the distance between two pillars must be in the range 10μm to 223μm to make a superhydrophobic surface when the surface of nylon pillars are covered by a low surface energy material such as fluoroamine. Figure 4 shows SEM images of the flocked surface of NF140. The fiber radii and heights are approximately 7 μm and 1 mm. Inter-fiber spacings were measured for adjacent fibers using Image J at 20 random locations. The distance between adjacent fibers ranged from 10 to 78 μm in Figure 4. According to Table 2, NF140 is expected to be superhydrophobic when the surface is grafted with 1H, 1H-perfluorooctylamine. Indeed, fluoroamine modified NF140 was superhydrophobic with water contact angles of 170° - 178°, as shown in Table 3.

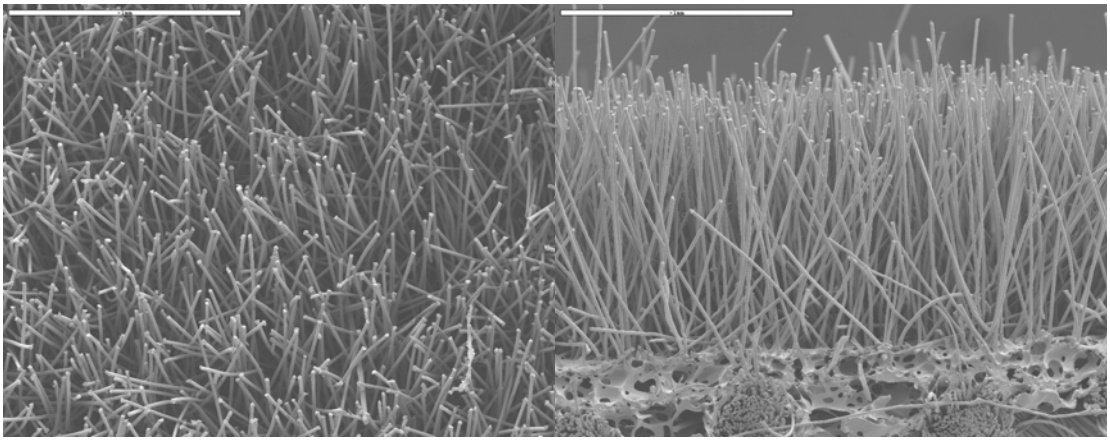

Figure 4. SEM view from above and from side of NF140 (50x).

Table 3. Comparison of predicted and measured apparent contact angles.

Sample	Apparent contact angle (degree)					
	Nylon		PAA grafted nylon		1H, 1H-perfluorooctylamine grafted nylon	
	Predicted	Measured	Predicted	Measured	Predicted	Measured
Film	72	$65 < \theta < 73$	$\theta < 72$	$43 < \theta < 50$	117	$93 < \theta < 110$
NF50	$\theta < 10$	$\theta < 10$	$\theta < 10$	$\theta < 10$	$138 < \theta < 180$	$132 < \theta < 140$
NF70	$\theta < 10$	$\theta < 10$	$\theta < 10$	$\theta < 10$	$150 < \theta < 180$	$168 < \theta < 175$
NF100	$\theta < 10$	$\theta < 10$	$\theta < 10$	$\theta < 10$	$157 < \theta < 180$	$170 < \theta < 178$
NF140	$\theta < 10$	$\theta < 10$	$\theta < 10$	$\theta < 10$	$150 < \theta < 180$	$170 < \theta < 178$

Table 3 shows the predicted and measured water contact angles for smooth nylon films and for the rough nylon structures made by flocking, and for all three surface treatments (untreated but cleaned, PAA grafted, and fluoroamine-grafted onto the PAA-grafted surface.) As mentioned earlier, a water droplet placed upon a smooth surface of nylon 6,6 should have a contact angle θ_e = 72º. According to the Wenzel equation, lower values of apparent contact angles are expected on rough surfaces when θ_e < 90º. For our rough surfaces, the water contact angles on nylon rough surfaces are predicted to be close to 0º. Indeed, rough surfaces made of nylon flock fibers absorb water into the flocked structure and the contact angles are less than 10° as expected. For the untreated nylon film and flocked fabrics the agreement between the predicted and measured contact angles is excellent (columns 2 and 3).

Upon treating the film surface with PAA, the water contact angle is expected to decrease. In the same manner, the water contact angles on a rough surface are expected to approach 0º. The PAA-grafted nylon rough surfaces absorb water into the flocked structure and the water contact angles of PAA grafted rough surfaces are less than 10°. Again, excellent agreement is found between the predicted values of the apparent contact angle and the measured values (columns 4 and 5 of Table 3) when the contact angle follows the Wenzel model and θ_e is less than 90°.

On the other hand, both the Wenzel and the Cassie-Baxter models predict that a rough surface becomes more hydrophobic when the contact angle on a flat surface is greater than 90°. Upon further treatment of the PAA-grafted nylon film with 1H, 1H-perfluorooctylamine, the contact angle of water on the flat film increases to θ_e = 93° - 110°. Thus the fluoroamine-grafted rough surfaces should be more hydrophobic ($\theta_r > \theta_e$) than the similarly treated films. This is exactly what is observed for all of our rough (flock) surfaces (columns 6 and 7 of Table 3). Samples NF70, NF100, and NF140 are all superhydrophobic ($\theta_r \geq 150°$) when the fluoroamine is grafted to the surface. For example, NF100 and NF140 have high apparent contact angles, 170° ~ 178°, and are superhydrophobic. Figure 5 shows a water droplet sitting on 1H, 1H-perfluorooctylamine grafted NF70. The water contact angle in this image seems to be 175°. Light can be seen between the droplet and a rough surface, which indicates that the water droplet is sitting on the top of flock fibers and follows the Cassie-Baxter model.

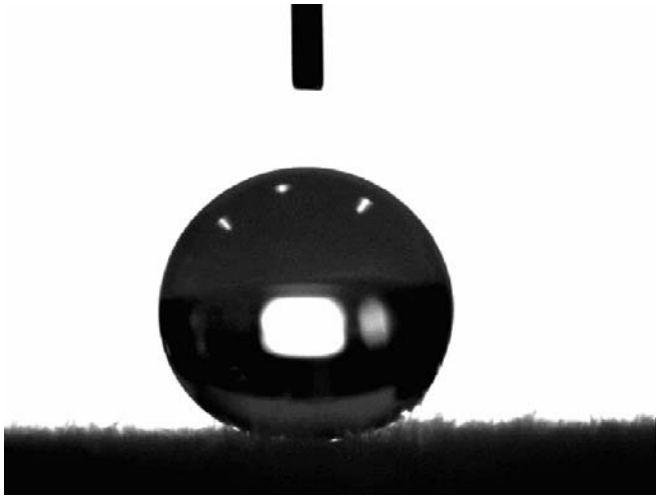

Figure 5. A water droplet on a superhydrophobic surface of NF70. Light under the droplet show that water is sitting on the top of the flock fibers.

Although θ_r for NF50 grafted with fluoroamine increases compared to the flat film, it does not become superhydrophobic since the measured distances in NF50 fall outside of the range required for a superhydrophobic surface. Indeed, the minimum apparent contact angle calculated from the Cassie-Baxter equation is 138° when the surface of NF50 is covered by fluoroamine. Again, there is excellent agreement between the predicted values of the apparent contact angle and the measured values.

Superhydrophobic surfaces were prepared at Ventana Research by treating the above nylon 6,6 fiber flocked polyester films with a dilute solution of polyisobutylene-alt-maleic anhydride (PIBMA). PIBMA was selected on the basis of its high chemical stability, presence of highly hydrophobic isobutylene repeat unit & anhydride repeat units present along its backbone. Unlike the former PAA polymer, the cyclic anhydride groups present within PIBMA were capable of readily reacting with residual amine groups present on the flocked nylon fiber surfaces and did not require the use of additional DMTMM to promote the grafting reaction. In addition, these cyclic anhydride groups also proved later to be suitable for grafting hydrophobic laurylamine and amine functionalized chloroaluminum phthalocyanine (AlPc) sulfonamide singlet oxygen generating photosensitizers upon the flocked fiber surfaces further enhancing its hydorphobicity and antimicrobial / decontamination properties respectively. Contact angle measurements were made upon PIBMA treated nylon film, fiber, and flocked polyester film surfaces using a Rame'-Hart Contact Goniometer. Wetting measurements were also conducted upon flocked specimens treated with PIBMA solution followed by surface reaction with laurylamine. The results from these wetting angle tests are summarized in the table below and are compared to conventional PAA treated materials.

Table 4. Wetting behavior of PIBMA treated Nylon 6,6 Film, Fiber, & Flocked Materials

Material	Wetting Contact Angle (degrees)
Water on Nylon Film	70
Water on PAA grafted Nylon Film	50
Water on Nylon Flocked Fabric	100-140
Water on PAA treated Flocked Fabric	0
Water on PIBMA grafted Nylon Film	72
Water on PIBMA grafted Flocked Fabric	95
Water on Laurylamine-PIBMA grafted Flocked Fabric	165-170

As can be seen from the results above, PIBMA treatment decreased nylon wettability. This was explicable on the basis that isobutylene functional groups present along the PIBMA graft copolymer became oriented at the air - fiber interface. The higher wetting contact angle associated with PIBMA treated nylon flocked fabric relative to planar nylon film suggested that Lotus effect wetting phenomena was occurring in the former specimen. Finally, post-treatment of PIBMA flocked nylon flocked fabric with laurylamine imparted superhydrophobic wetting characteristics upon the fabric. This was presumably attributed to the formation of fatty alkyl hemiamide reaction products along the fiber grafted PIBMA copolymer backbone. This demonstrated the utility of PIBMA and laurylamine grafts as an alternative fiber sizing material capable of imparting Lotus Effect Wetting behavior upon flocked fabric. LADM materials were

subsequently prepared via covalent grafting of protoporphyrin and phthalocyanine photosensitizers upon PAA and PIBMA grafted flocked fabric respectively.

Protporphyrin Based LADM Preparation & Characterization

A similar process was employed by Prof. Michielsen at NCSU to prepare a protoporphyrin based version of light activated decontamination materials, LADM. These materials absorb visible light and convert oxygen from the air or dissolved in water to $^1\Delta_g$ oxygen. Since we wish to attach these materials to the same surface as above, we used the approach developed by Sherrill, Stojiljkovic and Michielsen [10]. The chemically bonded protoporphyrin IX, PPIX, and zinc protoporphyrin IX, Zn-PPIX, to the surface of nylon films and fabric using poly(acrylic acid), PAA, as a scaffold polymer.

Experimental:

Following the procedure described above, PAA was first adsorbed onto nylon fabric in the presence of coupling agent, DMTMM 4-(4,6-dimethoxy-1,3,5-triazin-2yl)-4-methylmorpholinium chloride). The PAA could not be removed in multiple washings. Next, an amide bond between the carboxylic acid groups in Zn-PPIX and the amino groups in ethylene diamine was formed by dissolving Zn-PPIX, ethylene diamine and DMTMM in water in a molar ratio of 1:2:2. The resulting product was isolated by column chromatography. The same approach was used to make the ethylene diamine derivative of Rose Bengal.

Next, the photocatalyst (Z-PPIX-g-ethylene diamine or Rose Bengal-g-ethylene diamine) were dissolved in water and grafted to PAA that had already been grafted to nylon, again using DMTMM as a coupling agent. After washing off excess photocatalyst and drying the fabrics, a portion was sent to Dr. Gordon Churchward (Emory U) for antimicrobial testing and to Dr. Robert Connors (WPI). The remainder of each fabric was tested for their ability to generate singlet oxygen.

A 500 watt ECD photoflood lamp was mounted 6 ft above the benchtop. A treated fabric was cut to a 6.5" diameter and placed in a custom built singlet oxygen test chamber. An o-ring was placed on the fabric to hold it in place and a second o-ring was place outside of the fabric to seal the chamber. The sealed chamber was filled with a fresh aqueous solution of 100 mM furfuryl alcohol and a dissolved oxygen sensor was attached. The apparatus was placed directly below the light source and the computer started reading the oxygen concentration. Finally, the light source was turned on and the light intensity was measured above the sample. Light intensity was 2.4 mW/cm^2. The dissolved oxygen concentration was recorded continuously until it dropped below 2 μM.

Results and Discussion:

The reaction of singlet oxygen with furfuryl alcohol removes oxygen from the sealed chamber. Thus the amount of singlet oxygen produced is equal to the amount of oxygen lost from they chamber. Figure 6 shows the loss of oxygen from the Zn-PPIX fabric and from a solution containing 5 μM Rose Bengal. Notice that the rate of singlet oxygen production is similar for both samples. Figure 6 shows similar data for all of the fabric samples made in this project.

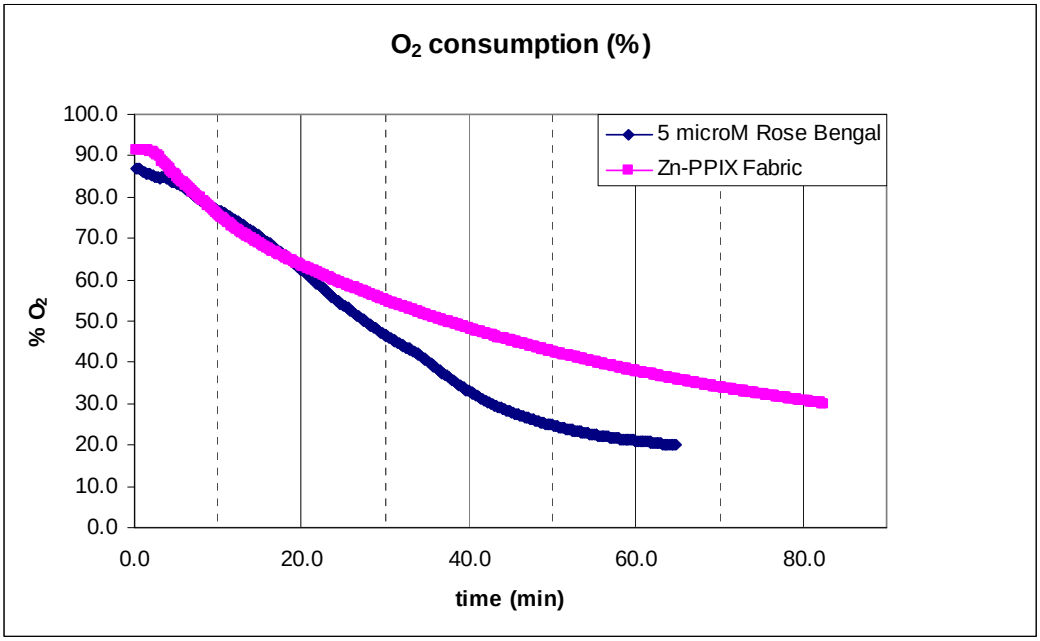

Figure 6. Loss of oxygen due to singlet oxygen production during photoexposure of a Zn-PPIX treated fabric and of a 5 μM solution of Rose Bengal.

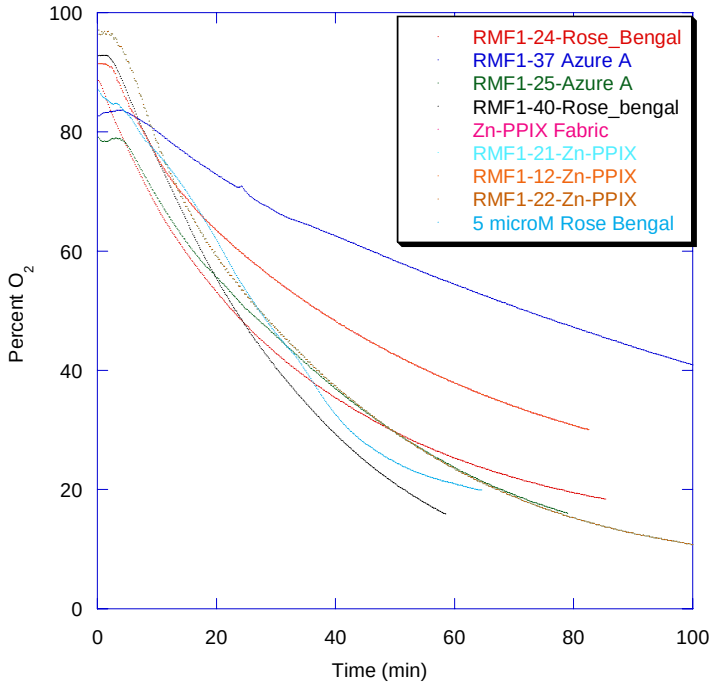

Figure 7. Loss of oxygen due to singlet oxygen production during photoexposure of treated fabrics and of a 5 μM solution of Rose Bengal.

Clearly, all of these treated fabrics produce large quantities of singlet oxygen upon exposure to visible light and air.

Aluminum Phthalocyanine Based LADM Preparation & Characterization

Similarly Ventana synthesized a series of LADM materials based upon chloroaluminum phthalocyanine (AlPc). AlPc was selected on the basis that, similar to protoporphyrin, it was well known for its ability to photogenerate singlet oxygen upon exposure to a combination of visible light and oxygen. Alkyl amine derivatives of AlPc were therefore synthesized via reaction between Dytek EP diamine & AlPc tetrasulfonylchloride according to the method detailed below. These aminated photosensitizers were later covalently grafted upon PIBMA copolymer.

Experimental:

Ventana prepared primary amine functionalized AlPc oligomer via reaction between duPont Dytek EP (1,3-pentanediamine) & aluminum phthalocyanine tetrasulfonyl chloride (AlPcTSCl).

In this case, AlPcTSCl reactant was first prepared by chlorosulfonating AlPc within neat chlorosulfonic acid (CSA) at 140 ^{o}C for 5 hours followed by cooling to 80 ^{o}C . $POCl_3$ was then added & the solution was stirred at temperature for 35 minutes. CSA was found to be reasonably effective at introducing sulfonyl chloride moieities on each of the four phenyl rings present on AlPc. Unfortunately, FTIR spectral analysis revealed that some of the substituents on the reaction product were sulfonic acid groups and were not all entirely substituted by sulfonyl chloride groups. This necessitated that the product be subsequently reacted with phosphorus oxychloride to ensure that complete conversion of the substituents to sulfonyl chloride groups. AlPcTSCl was then washed with several volumes of ice water, filtered, and vacuum dried over phosphorus pentoxide dessicant overnight.

Dry AlPcTSCl was then dissolved in 1.0 N methanolic KOH solvent. Methanolic KOH proved to be an superior solvent for AlPc tetrasulfonyl chloride compared to other known phthalocyanine solvents (i.e. pyridine, N-methyl-2-pyrrolidone, dimethyl sulfoxide etc.) since AlPcTSCl dissolved readily within the methanolic solvent at room temperature and yielded low viscosity solutions which were storage stable for several weeks. Dytek A was added dropwise to a stirred AlPCTSCl / methanolic KOH solution at room temperature followed by refluxing the reaction mixture for 3 hours. Dytek was reacted with AlPcTSCl in a 1:1 molar stoichiometry. A molar excess of KOH solute was also present in solution to trap the HCl which formed upon reaction of the amine with AlPCTSCl.

FTIR spectra obtained from the dried product indicted that it was essentially entirely composed of the desired sulfonyl chloride derivative as evidenced by the presence of strong sulfur-oxygen infrared absorption peaks between 1410 – 1380 cm^{-1} & 1204-1177 cm^{-1} respectively. No significant absorption was observed in the 1350- 1342 cm^{-1} & 1165-1150 cm^{-1} spectral range which would indicate the presence of sulfonic acid groups in the product. This indicated that the Dytek amine had reacted with the sulfonyl chloride substituent on AlPc. Sufficient water & KOH was then added to the reaction mixture to hydrolyze the remaining 3 moles of sulfonyl chloride on the Dytek amine substituted AlPc oligomeric photosensitizer to corresponding potassium sulfonate groups. The resulting aminated AlPc oligomer was then reacted with a solution of PIBMA polymer dissolved within 2-propanol solvent. The AlPc grafted polymer

solution was then applied to flocked nylon fabric surface via dip coating followed by drying the fabric sample under vacuum.

Amphiphilic AlPc derivatives were also synthesized by Ventana using a procedure similar to that above with the exception that ALPCTSCl was first reacted with one equivalent of laurylamine. This introduced a fatty lauryl hydrocarbon tail upon the AlPc photosensitizer. Portions of the fatty product were then covalently grafted upon PIBMA copolymer using Dyek EP diamine dissolved within aqueous alcoholic KOH solvent (See Fig. 8.). The remaining portion of synthesized fatty product was converted to low molecular weight anionic surfactant oligomer upon dissolution within aqueous KOH (See Fig. 9.). In both cases, KOH reacted and converted residual sulfonyl chloride groups attached to the phthalocyanine ring to corresponding potassium sulfonate moieties.

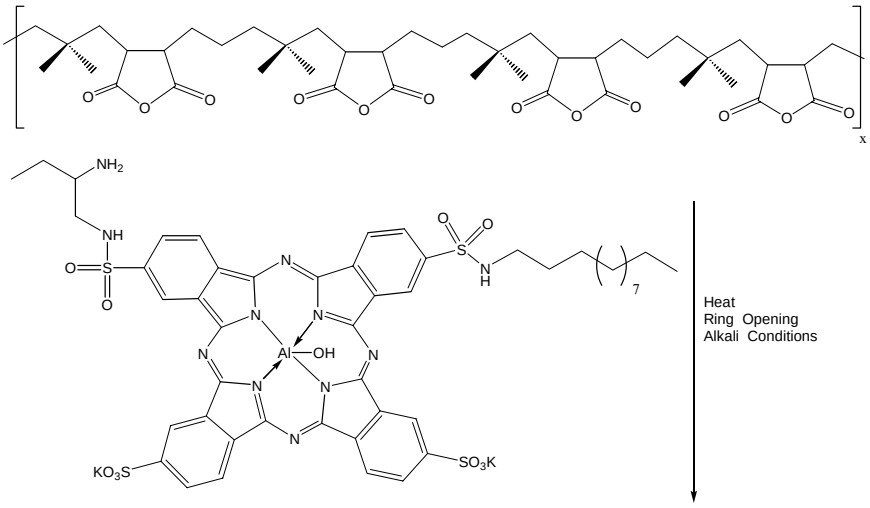

Figure 8. Covalent grafting of amphiphilic AlPc photosensitizer upon Polyisobutylene-*alt*-maleic Anhydride

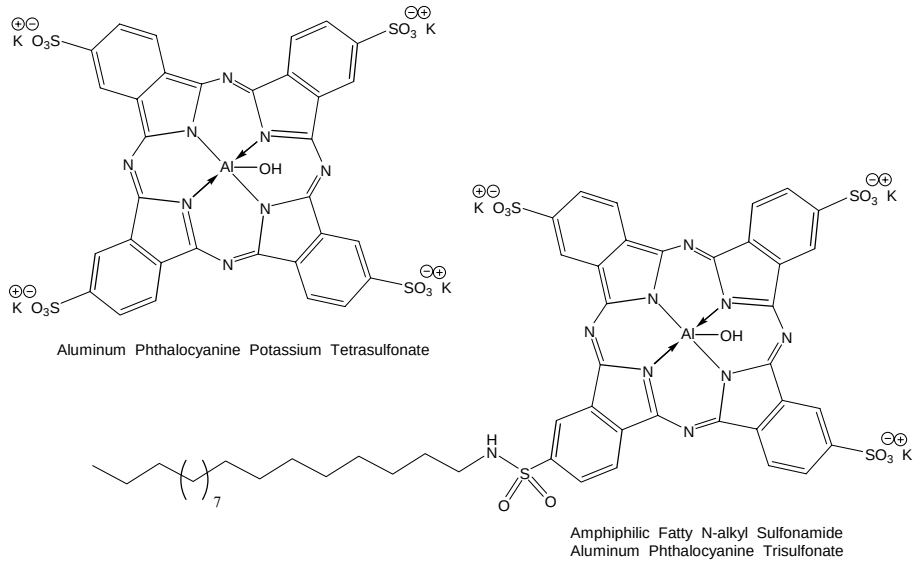

Figure 9. Structure of anionic aluminum phthalocyanine oligomer products synthesized by Ventana.

LOTUS-LADMs

In the final portion of this project, Lotus-LADMs were formed by first attaching the photoactive dye grafted polymers upon flocked fabric surface followed by grafting either laurylamine or fluoroamine to the same surface. These materials exhibited superhydrophobic wetting behavior and had the same color as the LADMs made above. The efficacy of these materials against biological toxins and chemical warfare simulants was then separately characterized by Profs. Churchward & Connors.

BIOLOGICAL TESTING

The efficacy of fabric treated with singlet oxygen photogenerators against *B. anthracis* spores was found to produce log 5.99 – 6.0 / cm^2 killing of germinated spores when illuminated by low intensities of visible light. These fabrics had little effect upon un-germinated anthrax. These results are discussed in detail below and suggestions are made for a future research direction for producing fabric treatment having significant activity against un-germinated spores.

Spore preparation. *Bacillus anthracis* Sterne was grown in DSM medium (Nutrient broth (Bacto) 8 g/L, KCl 1g/L, $MgSO_4$ 0.25 g/L supplemented with 1 mM $Ca(NO_3)_2$, 0.01 mM $MnCl_2$ and 1 μM $FeSO_4$) for 48 hours at 37ºC with shaking. At this time, by microscopic examination, the suspension contained <1% bacterial cells. The rest of the suspension was composed of highly refractile spores. The spores were centrifuged and suspended in water. This step was repeated four times. After the final wash the spores were suspended in a 20% w/v solution of renograffin (RenoCal-76, Bracco Diagnostics) and layered over a 50% w/v renograffin solution. The suspension was centrifuged at 10,000g for 20 minutes to pellet the spores. The renograffin and non-sedimenting contaminating material was removed by aspiration, the pellet was rinsed in water and then suspended in water at a concentration of ~10^{10} spores/ ml. Spore preparations were stored at 4ºC and monitored microscopically for signs of germination (transition to non-refractile dark appearance).

Illumination. 200 μl samples of spores containing ~2 x 10^7 spores were pipetted onto the surface of 2 cm^2 treated or control fabric sections in 35 mm cell culture dishes. The dishes containing spore-soaked fabric sections were placed below a Dyna-lume 'Dyna-Lite" illuminator (#240-351, Scientific Instruments Inc., Skokie, IL) and illuminated for various times with the light source at different vertical distances from the fabric. Light intensity was measured with a visible light meter (VWR Scientific). Following illumination, fabric sections were transferred to 15 ml conical polypropylene tubes containing 3 ml of water. The tubes were then vortexed for 10-15 seconds and left to soak for 5 minutes to release spores from the fabric.

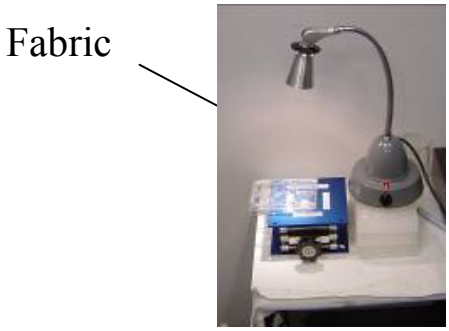

Figure 10. Apparatus employed for illuminating *B. anthracis* spores upon photosensitizer treated fabric.

Spore germination. In experiments where spores were exposed to germinant prior to illumination spores were incubated in LB broth (Lennox broth (Fisher Scientific) 20 g/L) for various times, then pelleted by centrifugation, and washed twice with water.

Viable count assay. Spore suspensions were diluted in water and plated on nutrient agar plates (Remel)**.**

Intensity of illumination. The following table shows some typical light intensities.

Surface	**Light Intensity (Lux)**
Laboratory bench	740
Office desk	550
Office window – no direct sunlight [a]	1,090
Exterior – no direct sunlight [a]	5,750
Exterior – direct sunlight [a]	50,000
Hospital emergency room – corridor [b]	660
Hospital emergency room – bed [c]	320
Hospital emergency room – curtain [d]	300

[a] – 9:00 a.m EST January 20, 2006. Clear sky.

[b] – Directly under fluorescent lighting, 3 feet from floor

[c] – Center of mattress

[d] – 3 feet from floor

Sporicidal activity of Zn-PPIX, N-Lauryl Al-Phthalocyanine & Azure A-Photosensitizer treated fabric.

Samples of fabric carrying singlet-oxygen generating compounds were exposed to a suspension of *B. anthracis* spores, then illuminated with a tungsten lamp (30,000 Lux) for different periods of time (0, 30, 60 90 and 120 min). The samples were then washed in 3 ml of water. Dilutions of these washings were plated to determine the number of viable spores. Results were normalized to a relative titer of 1.0 at zero time.

No statistically significant level of spore killing was observed using different times or intensities of illumination with either untreated or chemically treated fabric samples.

To determine if singlet oxygen could kill germinated spores, spores were incubated in broth for 120 minutes then washed with water. At 120 minutes of incubation in germinant, microscopic examination showed that >80% of the spores were germinated (non-refractile dark appearance), and the rest were either ungerminated (refractile bright appearance) or outgrown spores about to divide. The germinated spores were exposed to different intensities of illumination for 30 min. As shown below, 10 to 100-fold (ratio viable spores after illumination / viable spores without illumination: the zero illumination control was treated exactly the same as the other experimental samples except that it was not illuminated) killing was observed corresponding to a clinically significant level of surface decontamination. Applying the formula that has been used in the past (number of spores killed = number of viable spores in the treated sample subtracted from the

number of viable spores in the untreated sample) this corresponds to a log kill of 5.99-6.99 per cm^2. No statistically significant killing was observed for any control sample (fabric control, dark control).

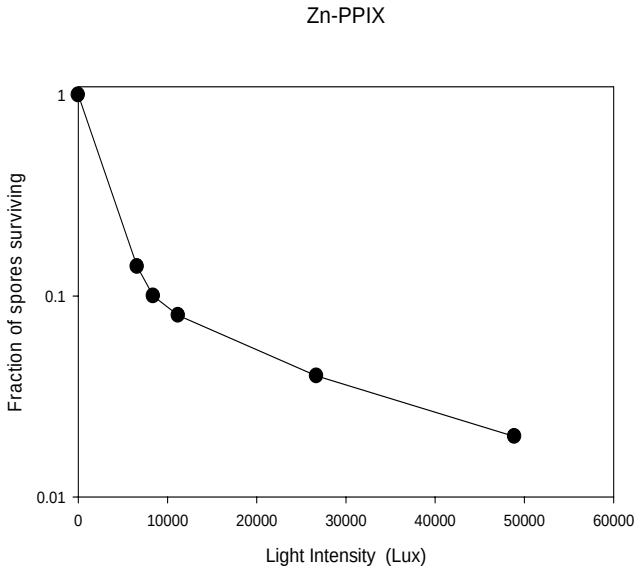

Figure 11. Killing efficiency of Zn Protoporphyrin treated fabric as a function of illumination intensity

It can be seen that the dose response curve is not linear and proportionally less killing is observed at higher illumination intensities. We believe that this is because oxygen is limiting in the small enclosed space used to hold the fabric. Experiments to determine if this is the case are under way.

To determine the minimum time of exposure to germinant, the spores were incubated in broth for different periods of time, washed then exposed on treated fabric to 6,600 Lux for 30 mins. As shown below, between 30 and 60 min exposure to germinant the cells become susceptible to killing by singlet oxygen.

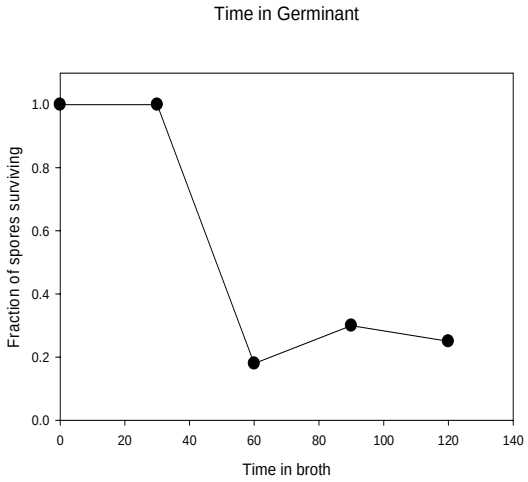

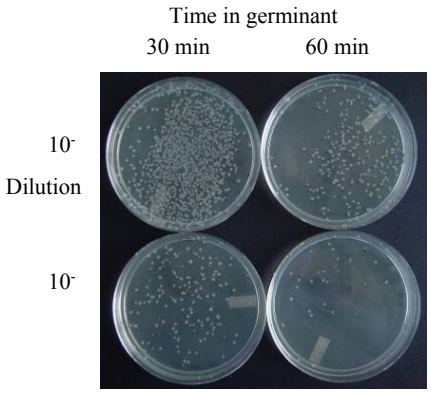

Conclusions

Fabrics carrying singlet oxygen-generating compounds can achieve clinically significant levels of decontamination of germinated spores of *B. anthracis*. Currently, decontamination is observed at levels of illumination equivalent to a clear January morning in Atlanta (latitude 33.6º N), shaded from direct sunlight. However, since the singlet oxygen-generating capacity of the fabrics is apparently being limited by the supply of oxygen, it is possible that similar levels of decontamination can be accomplished at light levels closer to those of ambient lighting, in a reasonable length of time. Experiments to test this possibility are currently underway. It is also possible that chemical disruption of the spore coat, rather than germination of the spores, can sensitize spores to singlet oxygen. A new class of compounds that might accomplish this goal is currently being tested.

Efforts were then directed by Ventana at synthesizing compounds which could adhere upon, cleave, & ultimately degrade *B. Anthracis* exosporia. Since the exosporia is responsible for protecting the anthrax DNA strands from environmental damage, degradation of the exosporia would presumably increase its permeability towards singlet oxygen and may provide a reasonable means for killing anthrax spores. A review of the literature indicates that the exosporia is primarily composed of unremarkable proteins crosslinked to each other via disulfide groups found on cystine amino acid protein repeat units. The stability of the exosporia has largely been attributed to the significant amount of cystine crosslinks present on its surfaces. Cleavage of these disulfide groups will therefore increase spore coat permeability and facilitate anthrax decontamination.

One plausible means of cleaving the disulfide linkages entails reducing cystine to cysteine via a base catalyzed reaction with monosubstituted thiols. In this case, the thiol undergoes an SN2 type nucleophilic displacement reaction with cystine forming a new disulfide linkage accompanied by the formation of cysteine (1, 2). This causes disruption of the exosporia crosslinks. (The proposed disulfide exchange reaction is depicted below.)

Figure 12. Disulfide exchange reaction between exosporia cystine crosslink & thiolate compound

In order to facilitate the above exchange reaction, it is necessary that the pKa of the exchanging thiol be higher than that of cysteine. (e.g. cysteine thiol group pKa $\approx$ 8.3). Therefore thiols having pKa values >> 8.3 should be sufficiently basic to undergo an exchange reaction with cystine (3, 4).

Several different classes of thiols were considered for this reaction. Besides having a high pKa value, suitable candidate compounds should have also exhibited bifunctional reactivity so that the thiol can ultimately be covalently attached to a flocked fiber substrate. Upon performing an exhaustive review of Chemical Abstracts literature, the following candidate compounds were selected for future evaluation: methyl thioglycolate, methyl 3-mercaptopropionate, thiolactic acid, thioglycolic acid, & mercaptopropyltrimethoxysilane. As a side note, it was interesting that these compounds have also found considerable utility in the past as depilatory agents due to their

ability to readily react with cystine linkages present in the keratinaceous components of hair. This supports the notion that they too may be effective against the keratin found on the anthrax exosporia. The reported pKa values for these compounds are presented in the table below. As can be seen all of these compounds have high pKa values coupled with the fact that they have other functionalities which enable them to be grafted onto textile fiber surfaces. A series of water dispersible graft and comb copolymers were synthesized from these thiol based precursors and were later evaluated as potential textile flock fiber sizings.

Candidate Exchangeable Thiol Derivative	**Reported pKa**
Methyl Thioglycolate	~ 9.8
Methyl 3-mercaptopropionate	10.6
Thiolactic acid	10.2
Thioglycolic acid	9.8
Mercaptopropyltrimethoxysilane	10.55

Gravimetric techniques were then used by Ventana to determine the ability of various aqueous alkaline thiol oligomers to promote swelling within keratin having chemical composition similar to *B. Anthracis* exosporia. The results from these experiments were summarized in the table below.

Table 5. Results for Swelling Experiments Performed upon Keratin Immersed within Various Aqueous Candidate Permeant Solutions

Permeant	**Concentration (M)**	**pH**	**Keratin Mass Change (%)**	**Swollen Keratin Appearance**
Guanidine Carbonate	2	10	No Change	Soft
Guanidinum 3-aminopentyl thiolactamide	1	10	414	Very Soft
Guanidinium thiolactate	2	9	249	" "
Guanidinum Thioglycolate	2	9	351	" "
Potassium 3-aminopentyl thiolactamide	2	10	201	" " Jelly-like
Potassium Thiolactate	4	6	39.1	Soft, Flexible
Potassium Thioglycolate	4	6	30.9	Minimal Change
Water		7	37.3	Somewhat Soft
Potassium Hydroxide	4	14	100 Dissolved	

Keratin underwent significant swelling in the presence of alkaline thiolactate and thioglycolate solutions relative to control. The type of cation present in these solutions also had an effect upon swelling whereby guanidinium was found to be more effective than potassium. This was understandable given the fact that guanidinum cations are known for their ability to readily disrupt hydrogen bonding within proteins [11]. In particular, guanidinium cations had a chemical structure which falls into a broad class of structures determined by Gordon & Jencks to denature proteins. (See Figure 13 below for structure of generic protein denaturing agents.)

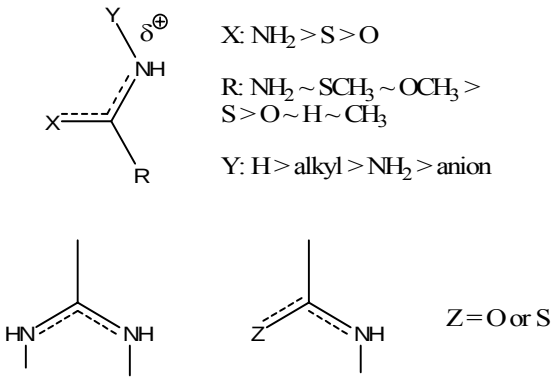

Figure 13. General chemical structural requirements for protein denaturant compounds (ref. 11)

It was also interesting to note that guanidine thiolates derived from 3-aminopentylthiolactamide induced greater swelling within keratin compared to corresponding salts prepared from thiolactic acid. This was explicable on the basis that the thiolactamide has a slightly lower pKa value compared to thiolactic acid (e.g. 8.2 versus 10.2 respectively) [12 - 17]. In comparison, thioglycolic has a reported pKa value of 10.2. The lower pKa value associated with the thiolactamide enables a higher concentration of thiolate species in solution capable of undergoing exchange reactions; disrupting the cystine disulfide crosslinks present within keratin. This combination of guanidinium cation coupled with thiolate anion is a potent agent against keratin whereby guanidinum cations disrupt protein hydrogen bonding while the thiolate cleaves the keratin crosslinks.

These results suggest that guanidinum thiolates may be capable of readily degrading keratin based anthrax exosporium coatings. Future work will focus upon covalent attachment of guanidinum 3-aminopentylthiolactamide functionalities upon aluminum phthalocyanine singlet oxygen photosensitizers. The resulting compound would be expected to readily permeate through the keratin in the spore coating while the photogenerated singlet oxygen would degrade its internal DNA & toxin generation capabilities.

Experiments were also conducted upon representative samples of the above solutions to determine verify their stability in the presence of singlet oxygen. A CAS literature search revealed that certain types of thiolate anion are capable of becoming degraded in the presence of strong oxidants. Solutions containing thiolate anion were then exposed to high concentrations of singlet oxygen to verify that they were unaffected. Discussion of the results of these experiments conducted is given below.

Sensitized irradiation of thioglycolic acid, thiolactic acid and their calcium salts with the presence of aluminum phthalocyanine sensitizer

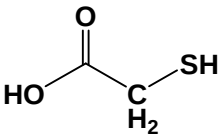

Thioglycolic acid

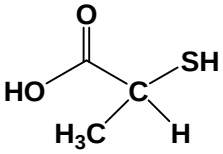

Thiolactic acid

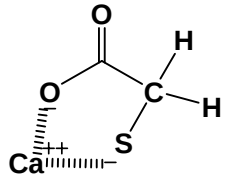

Calcium thioglycolate

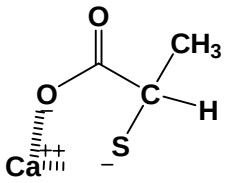

Calcium thiolactate

General procedure:

Solutions of thioglycolic acid and thiolactic acid in DMSO-d_6 and solutions of their calcium salts in D_2O with the presence of catalytic amount of aluminum phthalocyanine (AlPc) were irradiated by a Xenon arc lamp through a yellow filter for 60 min. Fine stream oxygen was bubbled to the solutions during irradiation. A red fluorescence was observed from solutions in DMSO-d_6 while solutions in D_2O (calcium salt solutions) were blue-purple and were difficult to indicate the red fluorescence.

All solutions were analyzed by ^{1}H- and ^{13}C-NMR spectroscopy before and after irradiation. Solutions of the calcium salts in D_2O with and without catalytic amount of aluminum phthalocyanine (AlPc) were left in the dark with O_2 bubbling for 60 min as control experiments.

In general, it was found that thioglycolic acid and its calcium salts were reactive towards singlet oxygen whereas corresponding thiolactates were unreactive towards it. NMR spectra of thiolactate derivatives before and after singlet oxygen exposure are discussed below. Figure 14 shows ^{1}H-NMR spectra of a solution of thiolactic acid/DMSO-d_6 + AlPc + O_2 before (top) and after irradiation (bottom). After 60 min of irradiation, the spectrum (bottom) revealed no spectral change or the formation of any product. Figure 15 shows ^{13}C-NMR spectra of the solution before (top) and after irradiation (bottom). After 60 min of irradiation, the spectrum (bottom) also revealed no spectral change or the formation of any new products.

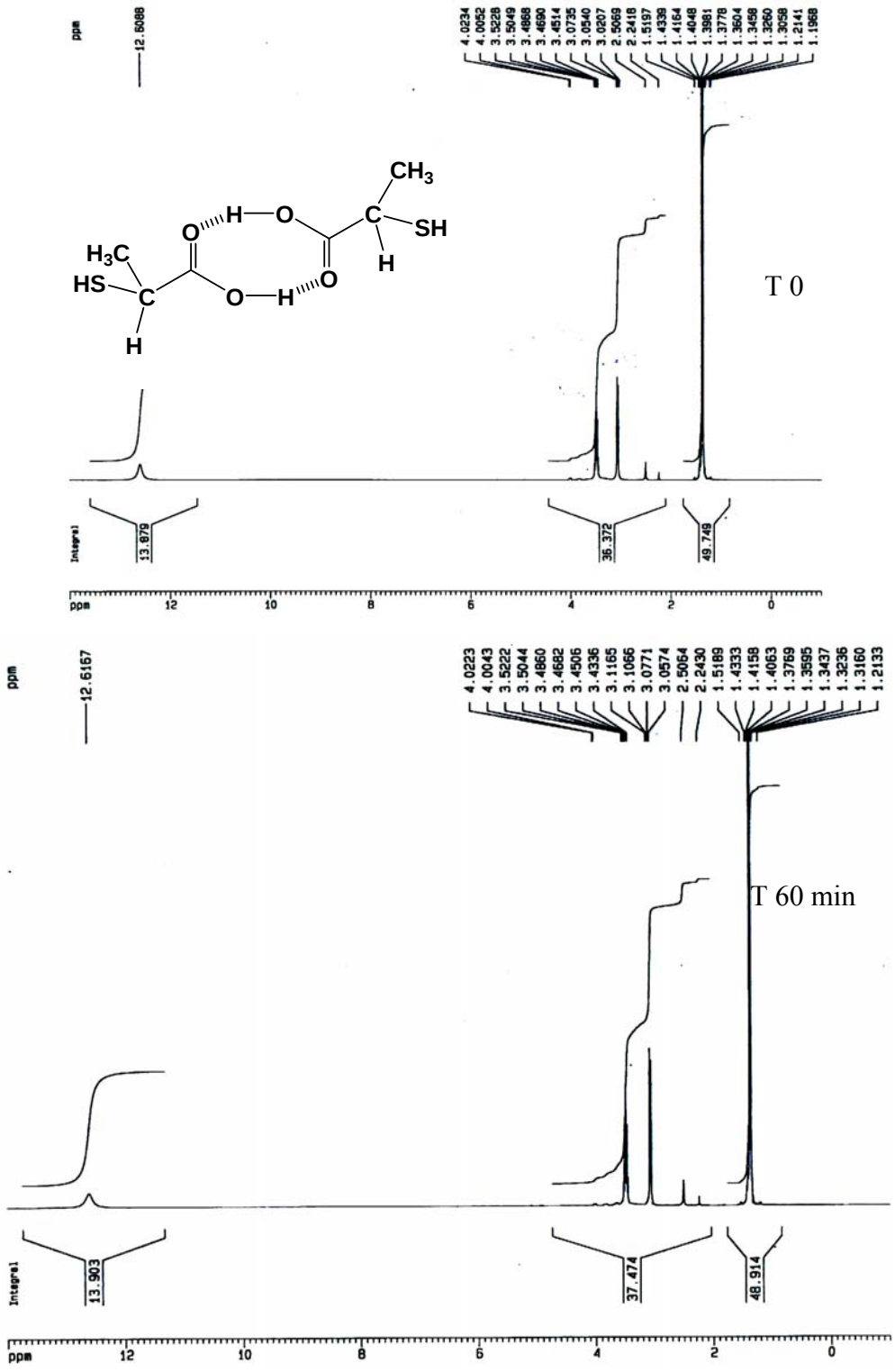

Figure 14. ^{1}H-spectra of irradiation of thiolactic acid/DMSO-d_6 + AlPc and O_2 bubbling

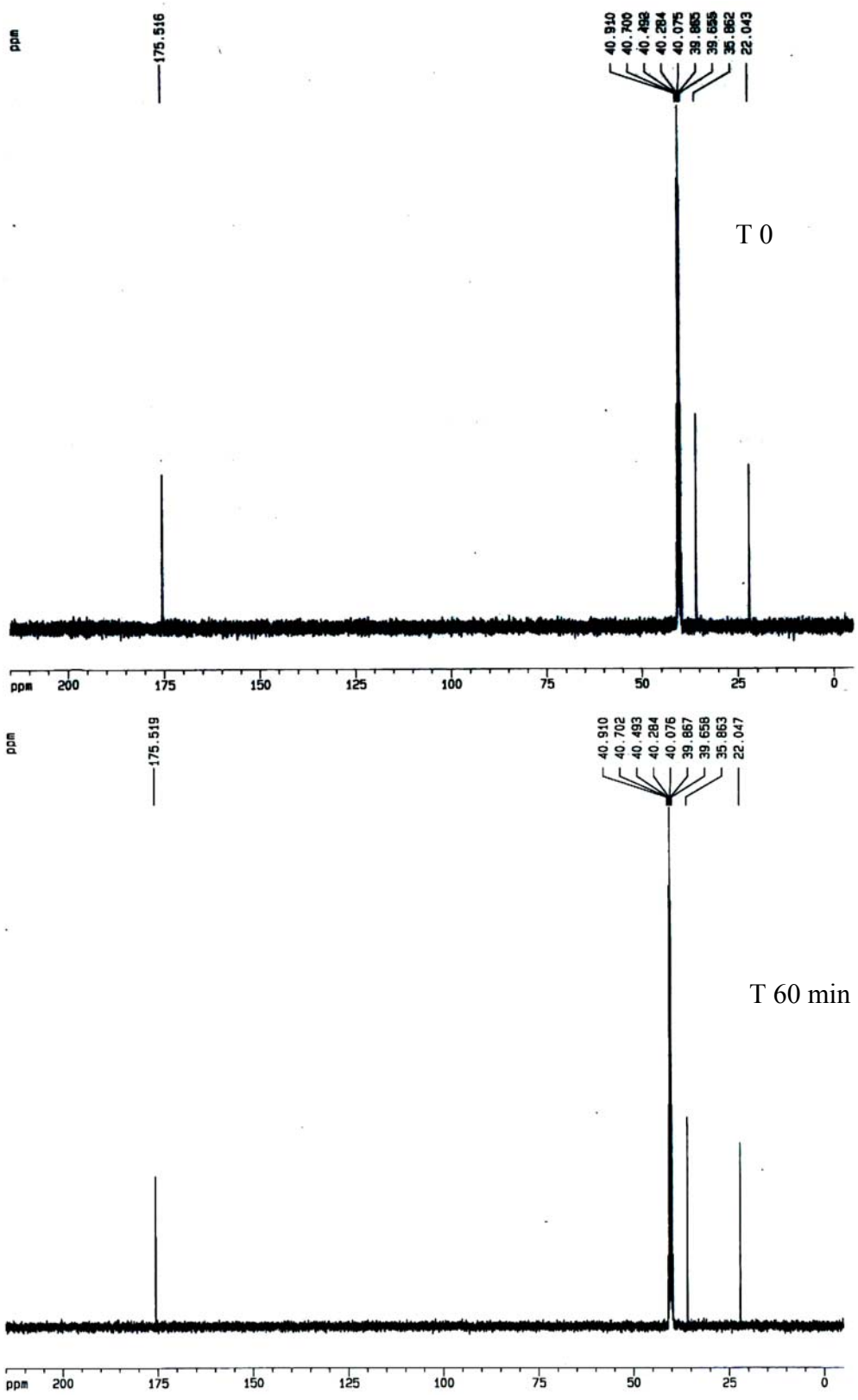

Figure 15. ^{13}C-spectra of irradiation of thiolactic acid/DMSO-d_6 + AlPc and O_2 bubbling

Irradiation of calcium thiolactate/D_2O + AlPc + O_2

Irradiation of a blue purple solution of calcium thiolactate/D_2O + AlPc + O_2 led to no color change from the original color before irradiation. The typical red fluorescence from Al-phthalocyanine sensitizer was difficult to identify in this case.

Figure 16 shows ^{1}H-NMR spectra of the solution before (top) and after irradiation (bottom). The spectrum before irradiation (top) showed two overlapping doublets at δ 1.18-1.38 and two multiplets at δ 3.21-3.27 **(X)** and 3.39-3.47 **(Y)**. The integration ratio of **X** : **Y** is 14.4. Since the α-carbon is a chiral center, thus the spectrum would indicate that the solution is a mixture of two enantiomers. The observed doublets would be due to $-CH_3$ couple to –CH and the multiplets would be due to the –CH couple to $-CH_3$. After 60 min of irradiation, the spectrum (bottom) shows that the signal integration ratio of **X** : **Y** decreases from 14.4 to 4.7. No evidence for formation of new products is observed. This would indicate that only enantiomeric ratio changes after irradiation.

Figure 17 shows ^{13}C-NMR spectra of the solution before (top) and after irradiation (bottom). After 60 min of irradiation, the spectrum reveals three new carbon-13 resonances at δ 17.8, 51.5 and 181.0. Based on ^{1}H-spectrum, the new observed peaks would be due to the carbon-13 resonances of the enantiomer not due to a new product.

Figure 18 and 19 shows ^{1}H-NMR spectra of the solutions with and without AlPc that were left in the dark with O_2 bubbling for 60 min. These control experiments showed enantiomeric ratio changes similar to the result observed under irradiation condition. The change was also observed in the only salt solution that was left in the dark with O_2 bubbling. This indicated that the observed change after irradiation would be due more likely to bubbling of O_2. However, explanation to this observation was unclear.

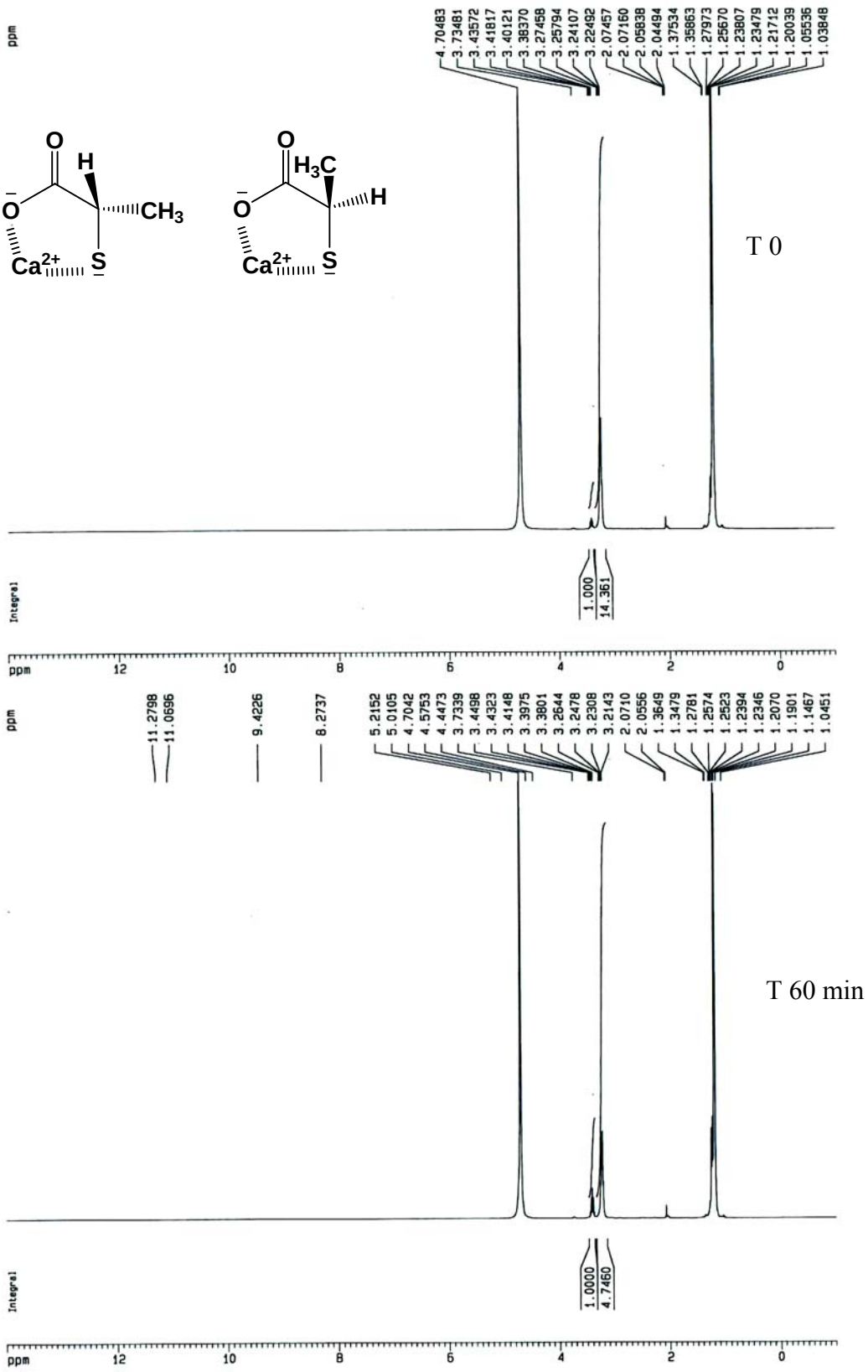

Figure 16. ^{1}H-spectra of irradiation of calcium thiolactate/D_2O + AlPc and O_2 bubbling

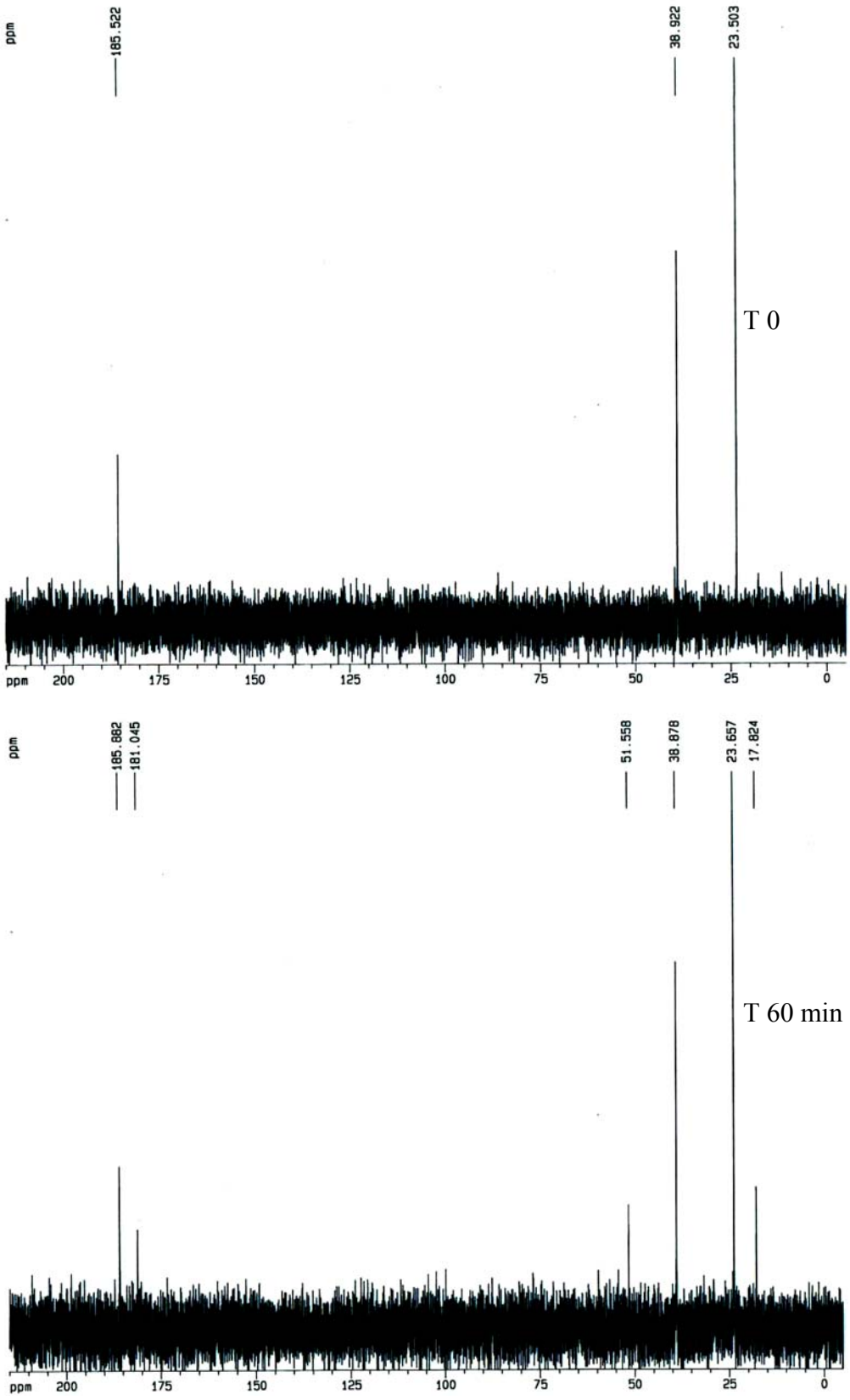

Figure 17. ^{1}H-spectra of irradiation of calcium thiolactate/D_2O + AlPc and O_2 bubbling

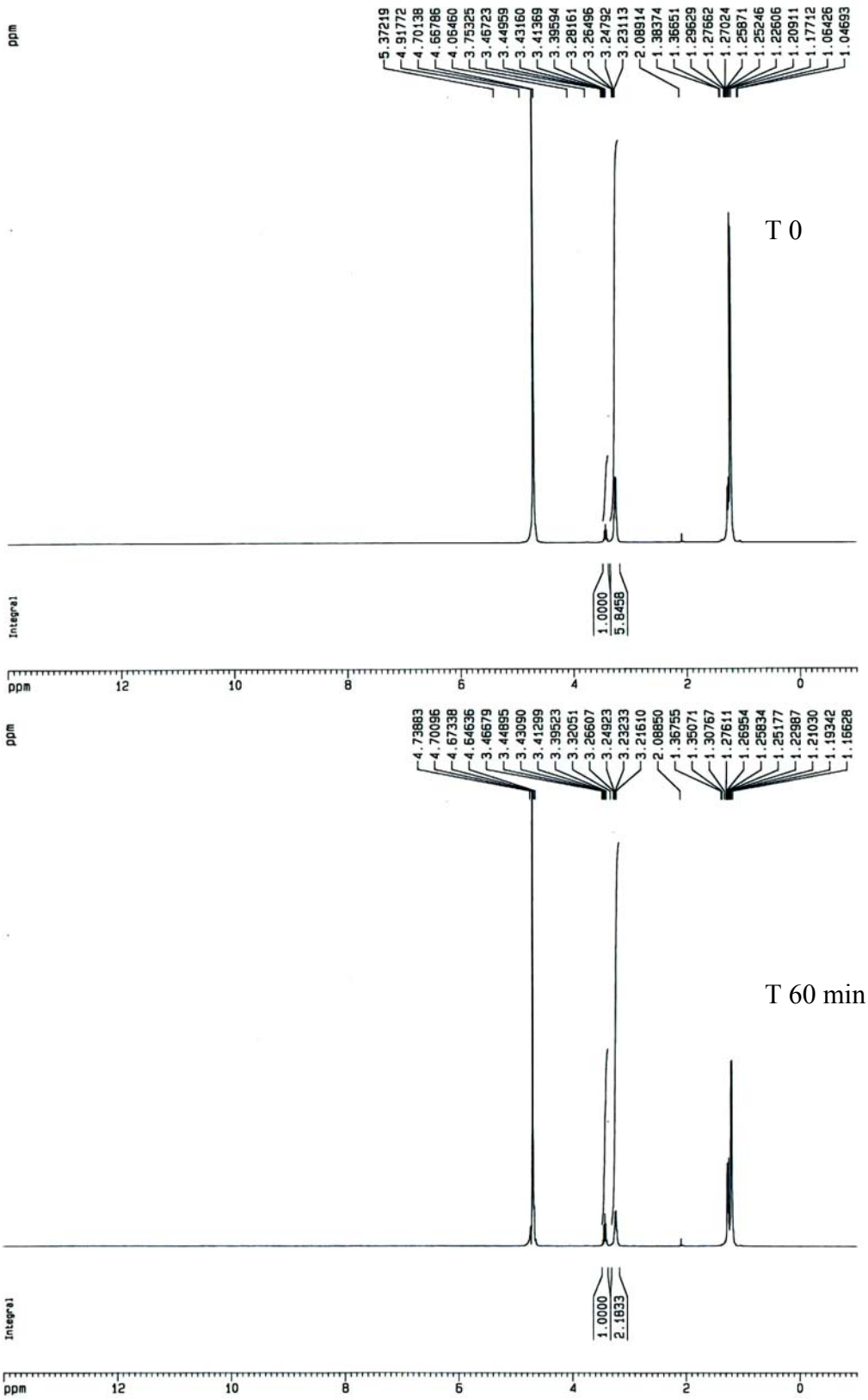

Figure 18. ^{1}H-spectra of calcium thiolactate/D_2O + AlPc and O_2 bubbling in the dark

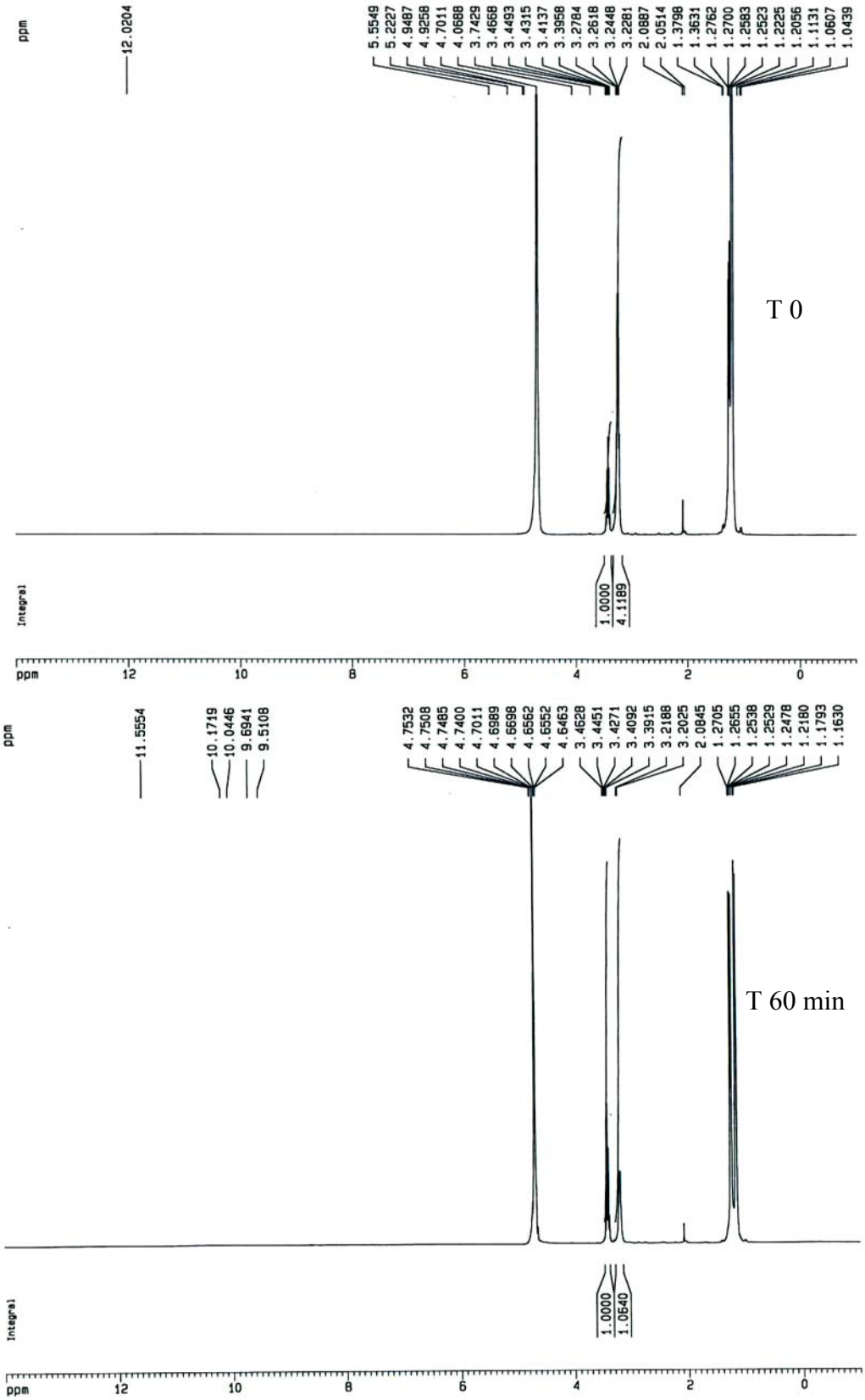

Figure 19. ^{1}H-spectra of calcium thiolactate/D_2O and O_2 bubbling in the dark

A series of thioamides were then synthesized at Ventana by aminolysis reaction between an amine and thioester or via direct amidation with a thio alkyl/aryl carboxylic acid. Thioamides were particularly attractive since the amide linkage provides a stable means of later coupling / attaching the thiol derivative to flock fiber surfaces.

Dytek A (1.3-pentanediamine) diamine was selected as a reactant for these aminolysis reactions since it primary amine endgroups differ significantly in reactivity from each other. This favored the formation of monosubstituted amide product; leaving the unreacted, somewhat sterically hindered primary amine endgroup on the oligomeric product. (Figure below depicts the synthesis of these amine terminated oligomers.)

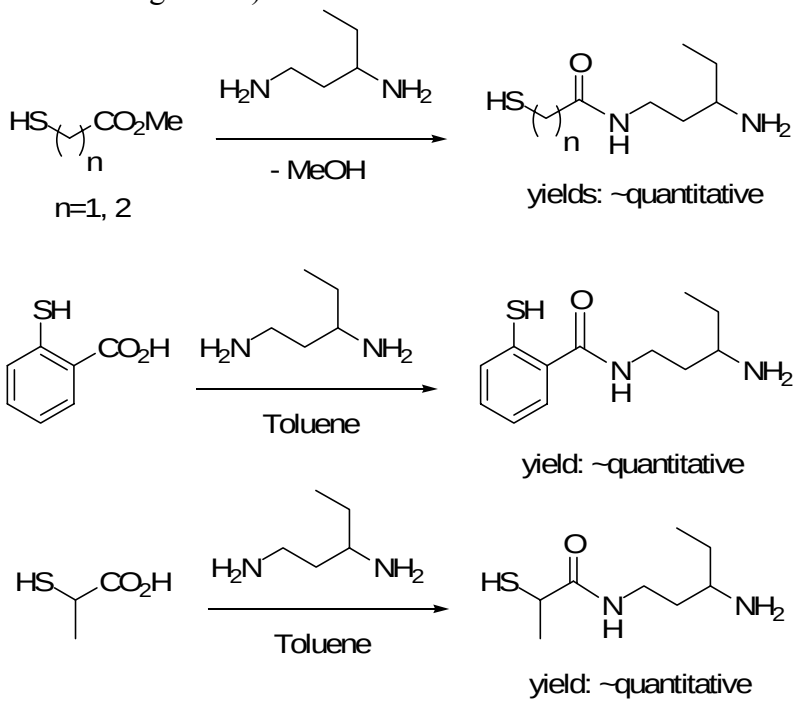

Figure 20. Synthesis of amine terminated oligomers bearing thiol functional groups.

Each of the amine terminated oligomers was then separately reacted with a Polystyrene – alt-maleic anhydride (SMA) copolymer. SMA was selected as a potential flock fiber sizing material given its reasonably hydrophobic character coupled the ability of its maleic anhydride repeat units to become covalently attached upon various flock polymer fiber surfaces. In particular, SMA copolymer was reacted with amine terminated oligomer in various stoichiometric ratios ranging from 30 – 70 mole percent. This left the remaining, un-reacted maleic anhydride repeat units on the copolymer available for subsequent reaction with flock fiber surfaces. (See Fig. below for depiction of reaction between SMA and amine terminated thioamide oligomer.)

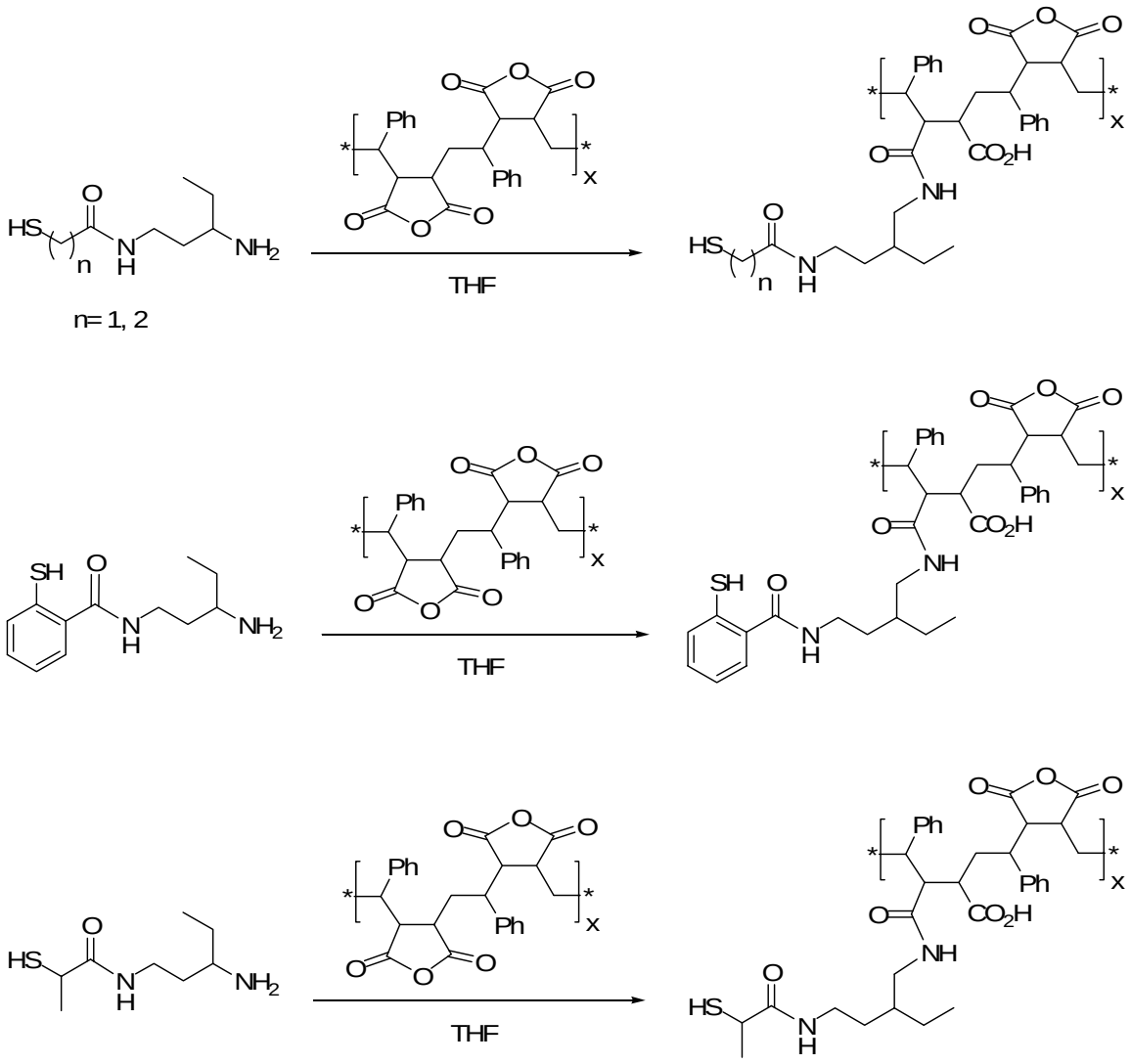

Figure 21. Synthesis of Flock Sizing Copolymer having thiol functionality

Oligomer having silyl ester functionality was also synthesized via reaction of methyl thioglycolate with aminopropyltriethoxysilane. (See Figure below for oligomer synthesis.) This compound differed from the former oligomers synthesized in that they had silyl ester endgroups which could be hydrolyzed and attached upon flock fibers via a hydrogen bonded siloxane network. Unfortunately this compound was highly hygroscopic and precipitated from solution upon standing.

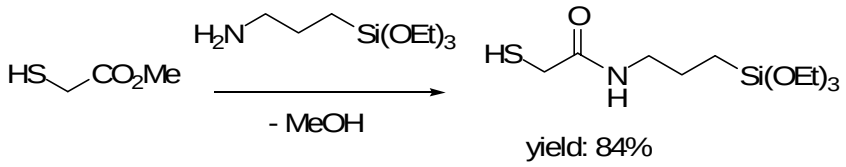

Figure 22. Synthesis of silyl ester endcapped thioamide compound

Finally oligomers having hydrophobic polydimethyl siloxane blocks were prepared via reaction between methyl thioglycolate and bifunctional, aminopropyl terminated polydimethylsiloxane polymer (PDMS) in a 1:1 molar stoichiometry. (See Fig. 23.) The resultant PDMS product therefore has both aminopropyl as well as thioglycolamide groups at each polymer end. Comb copolymers were then synthesized via reaction of SMA copolymer with the aminopropyl groups present on the PDMS –thioamide oligomers.

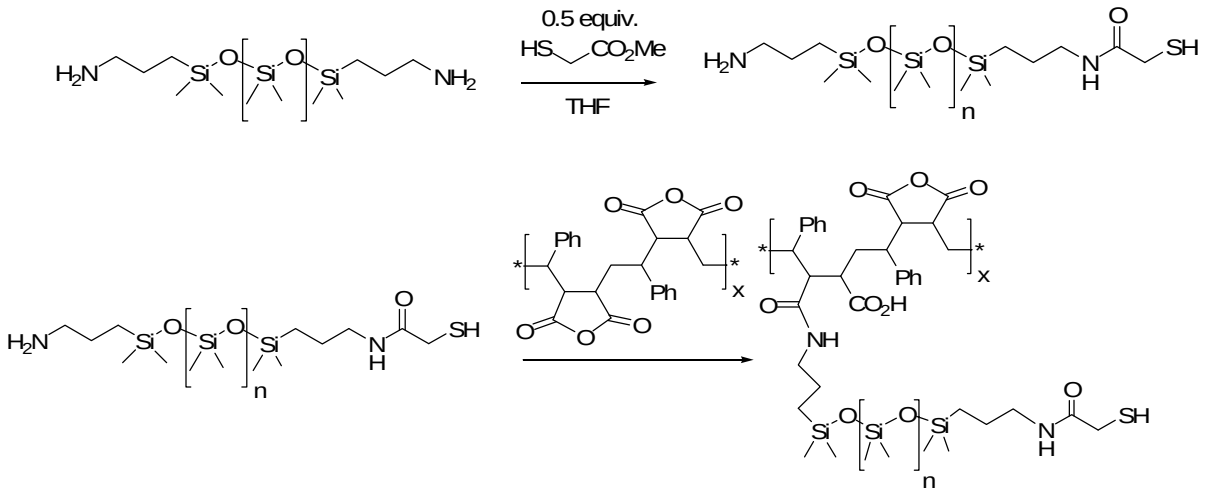

Figure 23. Synthesis of SMA sizing copolymer having hydrophobic, thioamide terminated dimethyl siloxane combs

Samples of keratin were immersed in each of the above oligomers and SMA derived copolymers depicted in Figures 20 - 23. Preliminary results suggested that each material rapidly wetted and induced significant swelling within keratin. Samples of guanidinium Dytek EP – thiolactamide reaction product were found to induce the greatest amount of swelling within the keratin test specimens and samples of this compound were subsequently sent from Ventana to Prof. Churchward to determine their efficacy against *B. Anthracis* spores. Preliminary tests conducted by Prof. Churchward indicated that this compound was effective in killing spores. Unfortunately the Phase I portion of the research program terminated before further work could not be conducted with this and related polymer grafted thiolactamide compounds. Overall these results suggested that deprotonated thiols could strongly interact and bind to *B. Anthracis* exosporia and could potentially be useful as sporicidal components within self-decontamianting superhydrophobic flock fiber coatings.

CONCLUSIONS

In order to render nylon 6,6 superhydrophobic, low surface energy materials, either 1H, 1H-perfluorooctylamine or laurylamine, were grafted onto smooth and rough surfaces of nylon 6,6, which were made by flocking. Water contact angles were measured. The rough surface became more hydrophobic than the corresponding flat surface when $\theta_e > 90°$ but more hydrophilic when $\theta_e < 90°$. Since nylon and PAA are hydrophilic, rough surfaces made of nylon or the PIBMA /

PAA grafted nylon absorbed water into the structures and both surfaces became more hydrophilic. However, the nylon rough surface grafted with a low surface energy material, (either laurylamine or 1H, 1H-perfluorooctylamine), became superhydrophobic ($\theta_r > 150°$) when inter-fiber distances between adjacent fibers fell within the ranges predicted by the Wenzel and the Cassie-Baxter models. Surfaces with water contact angles as high as 178° were made. Both mechanical and chemical surface modifications were required to make superhydrophobic surfaces.

In addition, photocatalytic dyes were attached to by woven nylon fabric and to nylon flock. The photocatalytic dyes attached to nylon generated singlet oxygen upon exposure to light. Materials which had been treated with both photocatalyst and fatty lauryl or perfluorinated amines exhibited superhydrophobic behavior.

Finally a new series of sporicidal compounds having thiolate functionality were synthesized. Preliminary results suggest that these compounds may have efficacy against *B. Anthracis* spores.

FUTURE WORK

Future research efforts could focus upon preparing LADMs having a combination of visible light activated photosensitizer along with thiolate functionalities. The thiolates would enable strong LADM binding upon exosporia while the photogenerated singlet oxygen would be capable of killing the treated spores.

ACKOWLEDGEMENTS

The authors wish to thank both Drs. Steven Wax & Stephen Lee from DARPA and the U.S. Army respectively for their kind financial support during this research program. In addition, Dr. Churchawin Changtong, a postdoctoral fellow in Professor Connors' group at WPI is acknowledged for his work in synthesizing and characterizing numerous porphryin & phthalocyanine based singlet oxygen photosensitizer - storage compounds. Drs. Peter J. Slavish and Bhaskar Tadikonda from Ventana Research are acknowledged for their work in synthesizing various thiolate, thiolactamide, and substituted phthalocyanine derivatives as well as their assistance in preparing superhydrophobic Lotus LADM flocked materials during this program. Dr. Rosario Fico and Ms. Hoon Joo Lee from NCSU are acknowledged for their work in preparing and characterizing LADM porphyrins as well as superhydrophobic Lotus LADM fabric materials. Finally Prof. Churchward at Emory Medical School is acknowledged for his work in determining LADM efficacy against a variety of pathogens including anthrax spores as well as both gram positive and gram negative bacteria.

REFERENCES

[1] Otten, A., Herminghaus, S. "How Plants Keep Dry: A Physicist's Point of View," *Langmuir* 2004, 20: 2405-2408.
[2] Barton, A. F. M. In *CRC Handbook of Solubility Parameter and Other Cohesion Parameters*; CRC Press: Boca Raton, 1983; Vol. 1, Chapter 17, pp 425-452

[3] van Krevelen, D. W.; Hoftyzer, P. J. In *Properties of Polymers*; Elsevier/North-Holland: New York, 1980; Vol. 2, Chapter 8, pp 166-172.
[4] Tobiesen, F. A., Michielsen, S. *J Polym Sci Part A: Polym Chem*, 2002, 40, 719-728.
[5] Thompson, K. F. Modification of Polymeric Substrates Using Surface-Grafted Nanoscaffolds. Ph.D. Thesis, Georgia Institute of Technology, Atlanta, GA, May 2005.
[6] Barton, A. F. M. In *CRC Handbook of Solubility Parameter and Other Cohesion Parameters*; CRC Press: Boca Raton, 1983; Vol. 1, Chapter 17, pp 425-452.
[7] van Krevelen, D. W.; Hoftyzer, P. J. In *Properties of Polymers*; Elsevier/North-Holland: New York, 1980; Vol. 2, Chapter 8, pp 166-172.
[8] Thompson, K. F., Michielsen, S. *J Polym Sci Part A: Polym Chem*, 2006, 44, 126-136.
[9] Patankar, N. A. *Langmuir*, 2003, 19, 1249-1253.
[10] Sherrill, J. Michielsen, S. Stojiljkovic, I. "The Grafting of Light Activated Antimicrobial Materials to Nylon Films" *J. Poly. Sci., Part A, Polymer Chemistry*, 2003, 41: 41-47.
[11] J. A. Gordon, W. P. Jencks, The Relationship of Structure to the Effectiveness of Denaturing Agents for Proteins, *Biochemistry*, *1963*, **2**, 47-57.
[12] J. W. Haefele and R. W. Broge, *Kosmetik-Parfum-Drogen Rundschau*, 8, 1-4 (1961)
[13] R. S. Saxena and P. Singh, *J. Indian Chem. Soc*., 47 (1), 1076-80 (1970)
[14] "The Measurement of **Thiol**-Disulfide Interchange Reactions and **Thiol** **pKa** Values", Houk, J., Singh, R. and Whitesides, G. M., in *Methods in Enzymology: Sulfur and Sulfur Amino Acids*, W. B. Jakoby and O. W. Griffith, Eds., *Academic Press*, **New York**, *1987*, 129-143.
[15] "Structure-Reactivity Relations for **Thiol**-Disulfide Interchange", Houk, J. and Whitesides, G. M., *J. Am. Chem. Soc.*, **1987**, *109*, 6825-6836
[16] "Activation Parameters for Thiolate-Disulfide Interchange", Whitesides, G. M., Houk, J. and Patterson, M. A. K., *J. Org. Chem.*, **1983**, *48*, 112-115.
[17] Rates of **Thiol**-Disulfide Interchange Reactions Involving Proteins, and Kinetic Measurements of **Thiol** **pKa** Values", Shaked, Z., Szajewski, R. P. and Whitesides, G. M., *Biochemistry*, **1980**, *19*, 4156-4166.

APPENDIX A

LOTUS-LADM BASED SELF DECONTAMINATING SURACES
Contract # W911NF-04-C-0081

ADDITIONAL BIOLOGICAL TESTING UPON GRAM (+/-) BACTERIA

Samples of ZnPPIX & AlPc tetrasulfonate treated fabric were provided to Prof. Churchward at Emory University Medical School by NCSU and Ventana respectively to determine their efficacy at decontaminating against *Staphylococcus aureus (Gram Positive bacteria), E. Coli (Gram Negative bacteria)* pathogens.

The testing protocol used 4 cm^2 samples of photosensitizer treated textiles whereby a textile sample was first placed in 3 ml of suspended microorganisms, then removed and placed in a sterile dish. The sample was illuminated with 60,000 lux from an incandescent lamp for 30 mins. (This level of illumination corresponds to full sunshine at 4:00 pm in late January in Atlanta (latitude 33° N).) Two controls were performed: 30 mins incubation without illumination, and 30 mins illumination of textile samples without grafted photoactive compounds. The textile samples were then washed in 3 ml of sterile buffer and the number of microorganisms determined by serial dilution and plating. The following results were obtained:

Staphylococcus aureus:

LADM	PPIX
Survival	10^{-3}
Input	$3x10^7$
Log kill	7.47

Even though ZnPPIX photosensitizer was effective against S. Aureus bacteria, it proved ineffective against Gram Negative bacteria. Attempts to kill S. Aureus with tetrasulfonated AlPc photosensitzer also proved unsuccessful. This was not entirely surprising since a review of the literature indicates that both neutral & anionic charged photosensitizers do not significantly interact with the outer membrane of gram negative bacteria and hence were ineffective at killing the bacteria.

Bacterial samples were then retested by Emory using amphiphilic fatty N-alkyl sulfonated AlPc photosensitizers previously synthesized by Ventana. (See Figs. 8 & 9 in the report above for the amphiphilic AlPc photosensitizer chemical structure). The amphiphilic version of AlPc was found to be highly effective against *E. Coli 0157H7* Toxin Negative Strain. Log 7 Kill values were obtained upon irradiating bacterial strains for 30 minutes using a 60, 000 lux intensity incandescent lamp.

These results were significant since this photosensitizer was not predicted by the literature to exhibit any efficacy against gram negative bacterial strains. This also suggests that suitable photosensitizers should not only be efficient singlet oxygen producers but they should also strongly adsorb / interact with the surface of the pathogen undergoing decontamination.

Evidently the introduction of a fatty hydrocarbon tail onto the AlPc enabled the photosensitizer to have greater interaction with the outer membrane of E. Coli and killed the bacteria. This result was significant since the authors are unaware of any literature suggesting the efficacy of anionic amphiphilic photosensitizers against this type of bacteria.

APPENDIX B

LOTUS-LADM BASED SELF DECONTAMINATING SURACES
Contract # W911NF-04-C-0081

DEVELOPMENT OF DUAL SINGLET OXYGEN PHOTOSENSITIZER – STORAGE COMPOUNDS

A series of novel compounds were also synthesized and characterized during this program were capable of photogenerating as well as reversibly trapping / releasing singlet oxygen upon exposure to a combination of visible light and ambient oxygen. These compounds were primarily based upon pyridone derivatives covalently linked to porphyrin photosensitizers. In this case, singlet oxygen produced by porphyrin photosensitization became trapped by an adjacent pyridone moiety forming an endoperoxide complex. The endoperoxides were thermally unstable and were found to reversibly revert back to pyridones upon standing in darkness. This ultimately extended the utility of these photosensitizers for use in both light and dark decontamination situations. Since these compounds were developed towards the end of the program, time did not permit their evaluation as LADMs upon flocked superhydrophobic surfaces. The development of these materials is discussed in greater detail below.

2-Pyridones as singlet oxygen storages

Various N-substituted-2-pyridone singlet oxygen trapping compounds were synthesized according to the synthetic route shown in Scheme 1.

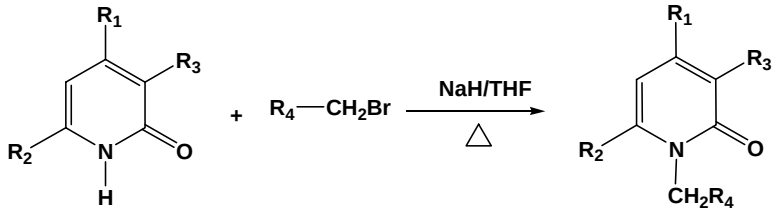

1; $R_1 = CH_3$, $R_2 = H$, $R_3 = H$, $R_4 = Ph$

2; $R_1 = H$, $R_2 = CH_3$, $R_3 = H$, $R_4 = Ph$

3; $R_1 = H$, $R_2 = H$, $R_3 = CH_3$, $R_4 = Ph$

4; $R_1 = H$, $R_2 = H$, $R_3 = H$, $R_4 = Ph$

5; $R_1 = H$, $R_2 = H$, $R_3 = H$, $R_4 =$ p-CNPh

6; $R_1 = H$, $R_2 = CH_3$, $R_3 = H$, $R_4 =$ p-CNPh

7; $R_1 = H$, $R_2 = CH_3$, $R_3 = H$, $R_4 = CH_3(CH_2)_5$

8; $R_1 = H$, $R_2 = CH_3$, $R_3 = H$, $R_4 = CH_3CH_2$**CO**

Scheme 1

Water soluble N-substituted-2-pyridones were also synthesized as summarized in Scheme 2. It should be noted that the pyridone **10** and **21** were fairly soluble in water at neutral as well as alkaline pH values.

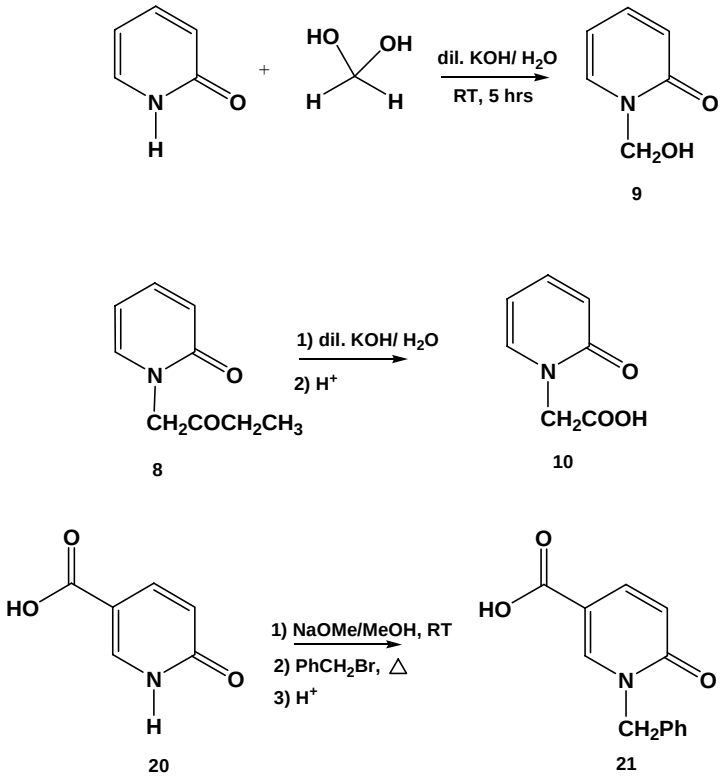

Scheme 2

Pyridones **1-9** were tested for their capacity to trap, store and release singlet oxygen in $CDCl_3$ under visible light irradiation while employing TPP (tetraphenylporphyrin) or AlPC (Aluminum phthalocyanine) as a photosensitizer. Scheme 3 shows the corresponding endoperoxides formed from singlet oxygen trapping of pyridones **1-9**. The trapping and releasing process was monitored using ^{1}H-NMR spectroscopy. Formation of endoperoxides from these pyridones was verified in the ^{1}H-NMR spectra of the reaction mixture via monitoring characteristic absorptions of the diasteriotropic methylene protons bonded to the nitrogen atoms of the pyridone rings. (as labelled by * in Scheme 3.) In all cases except endoperoxide **8**, the methylene protons of the endoperoxide products appeared as two doublets with large coupling constants (~ 15 Hz). In the endoperoxide **8**, the methylene protons bonded to the nitrogen atom of the pyridone ring appeared as a multiplet.

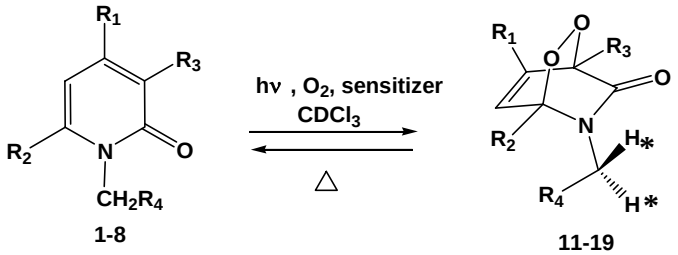

1-8 **11-19**

11; $R_1 = CH_3$, $R_2 = H$, $R_3 = H$, $R_4 = Ph$

12; $R_1 = H$, $R_2 = CH_3$, $R_3 = H$, $R_4 = Ph$

13; $R_1 = H$, $R_2 = H$, $R_3 = CH_3$, $R_4 = Ph$

14; $R_1 = H$, $R_2 = H$, $R_3 = H$, $R_4 = Ph$

15; $R_1 = H$, $R_2 = H$, $R_3 = H$, $R_4 = p\text{-}CNPh$

16; $R_1 = H$, $R_2 = CH_3$, $R_3 = H$, $R_4 = p\text{-}CNPh$

17; $R_1 = H$, $R_2 = CH_3$, $R_3 = H$, $R_4 = (CH_2)_5\mathbf{CH_3}$

18; $R_1 = H$, $R_2 = CH_3$, $R_3 = H$, $R_4 = COCH_2CH_3$

19; $R_1 = H$, $R_2 = H$, $R_3 = H$, $R_4 = OH$

Scheme 3

Table 1 shows relative ratio of endoperoxides formation after irradiation using AlPc sensitizer. The results show that endoperoxide **18** was the most reactive toward singlet oxygen trapping.

Table 1

Time (min)	**Relative ratio of endoperoxides formation after irradiation**								
	11	**12**	**13**	**14**	**15**	**16***	**17**	**18**	**19**
40	0.03	*0.14*	0.03	0.04	0.02	-	0.04	0.05	0.05
160	0.09	*0.34*	0.10	0.8	0.06	-	0.13	0.45	-
240	0.12	*0.40*	0.14	0.10	0.08	-	-	-	0.23
360	-	-	-	0.15	0.11	-	0.19	0.70	-

* Endoperoxide formation was identified but no data as the function of time available.

The endoperoxides were heated at 40 or 50 °C which led back to the original pyridones. This reversible trapping and releasing process could be operated in number of cycles without side reactions or decomposition for all pyridones studied.

Endoperoxide decomposition kinetics of some endoperoxides (**14**, **17** and **18**) were performed at various temperatures. Table 2 shows kinetics decomposition data of the endoperoxide **14**, **17** and **18**. This table reveals that kinetic parameters of the endoperoxide decomposition process in **14**, **17** and **18** are similar. This indicated that the substituted groups at nitrogen atom of the endoperoxide rings did not inhibit or interfere with endoperoxide decomposition and the release of singlet oxygen.

Table 2

Endoperoxide	$\Delta H^{\neq}$(kcal/mol)	$\Delta S^{\neq}$(cal/mol K)	$\Delta G^{\neq}$(kcal/mol)
14	26.30±0.05	6.89±0.16	24.20±0.05
17	25.44±1.43	5.66±1.10	23.75±1.07
18	26.40±1.18	5.89±3.70	24.60±1.10

Although, the kinetics decomposition of the endoperoxides bearing substituents on the endoperoxide ring (such as **11-13**) were not studied. Experimental results showed that these endoperoxides with methyl substituted at various positions on the ring (**11-13**) decomposed slowly at T < 40 °C with the similar rates to **14** (the unsubstituted). These results were very encouraging since it enabled these materials to function near room temperature.

Pyridones **10** and **21** were tested for their capacity to trap, store and release singlet oxygen within D_2O solvent under visible light irradiation employing **$TPPSCl_2$** (sulfonated TPP), **MB** (methylene blue) **TPPCOONa** (tetraphenylporphyrin tetracarboxylate) as a photosensitizer. Scheme 4 shows the expected endoperoxides (**22** and **23**) formed from singlet oxygen trapping of pyridones **10** and **21**. In the case of pyridone **10**, the results showed that irradiation of this pyridone in D_2O with the presence of **MB** led to the formation of a new product which the ^{1}H-spectrum revealed the characteristic two doublets with a large coupling constant corresponding to the previous observed endoperoxide formation. However, the formation of this product was observed in a trace quantity after > 12 hrs of irradiation. After heating at 50 °C, the ^{1}H-spectrum showed consumption of these two new doublets and recovery of the starting material. Irradiation of the carboxylate form of pyridone **10** in NaOD/D_2O was performed under the same condition. The ^{1}H-spectrum showed the formation of a new product which did not correspond to the previously observed endoperoxide. The formation of this product was not identified. Irradiation of the pyridone **21** or its carboxylate form in D_2O or NaOD/D_2O with the presence of **$TPPSCl_2$** or **TPPCOONa** led to the formation of a new product which did not correspond to the previous observed endoperoxide formation. However, irradiation of the pyridone **21** in $CDCl_3$ with TPP sensitizer led to the formation of a new product whereby its ^{1}H-spectrum corresponded to the formation of the endoperoxide formation. This product decomposed after heating at 50 °C leading to recovery of the starting pyridone **21**. It should be noted, however, that the endoperoxide formation from the pyridone **21** in $CDCl_3$ was observed in a small amount after > 11 hrs of irradiation. These results would suggest that constructing water soluble pyridones containing a carboxylic functional group could lead to the trapping of singlet oxygen as their endoperoxide derivatives but the rate of endoperoxide formation would be very slow compared to the trapping of the other pyridones in $CDCl_3$. Irradiation of their carboxylate forms under sensitization condition in NaOD/D2O does not give the corresponding endoperoxides.

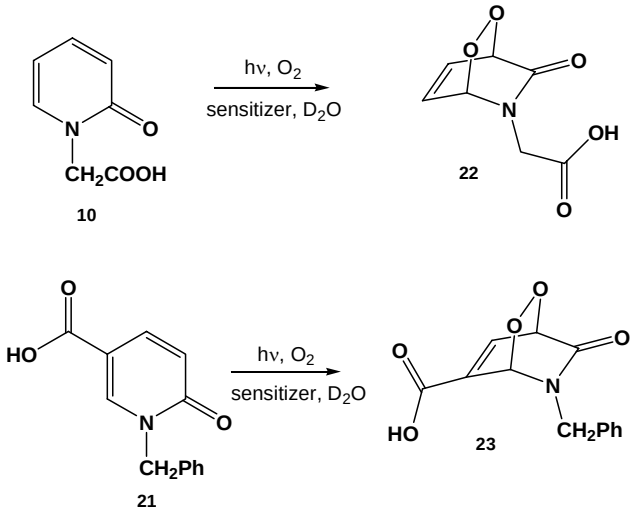

Scheme 4

Pyridones link Zn-phthalocyanine

Linkage of pyridones upon un-metalated Phthalocyanine **(27)** & Zn-phthalocyanine **(26)** was attempted according to the synthetic route outlined in Scheme 5 below.

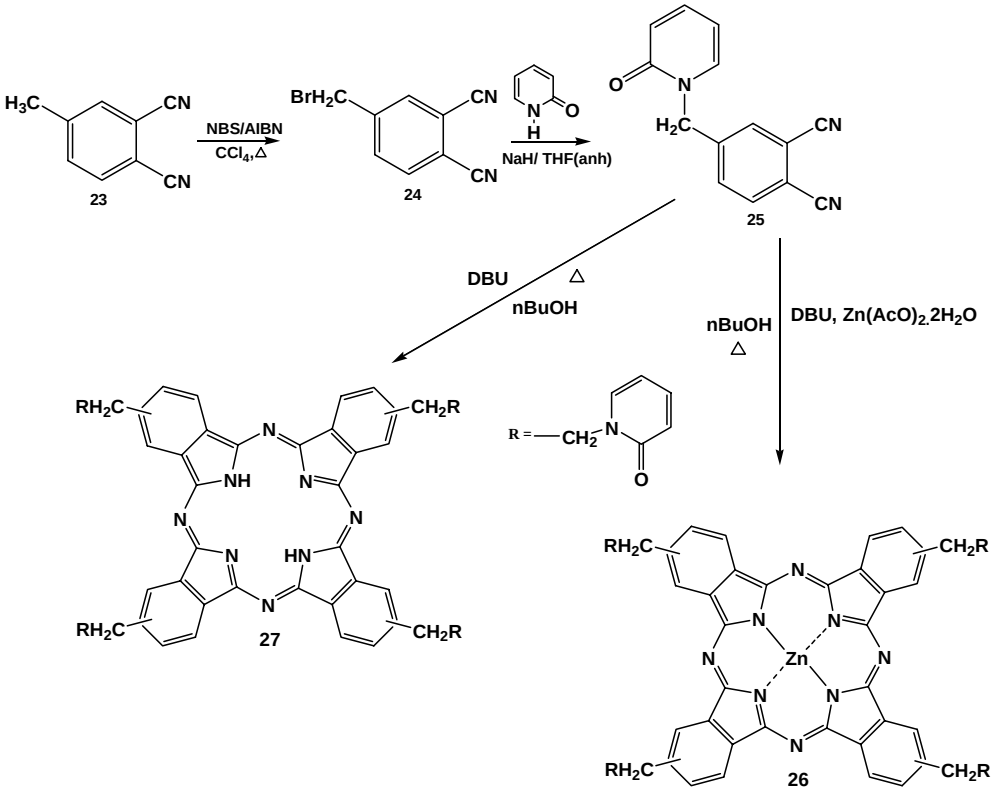

Scheme 5

Basic catalyzed cyclization of **25** in refluxing nBuOH with the presence or absence of $Zn(OAc)_2.2H_2O$ gave blue solid materials (named **BS1** and **BS2**, respectively). Both blue solids were insoluble in water and poor soluble in most organic solvents. UV-Vis of **BS1** and **BS2** could be recorded in DMSO while the ^{1}H-spectrum was recorded only for **BS1** in DMSO-d_6. Both **BS1** and **BS2** exhibited broad strong absorption bands in the region of 500-750 nm while an authentic sample of ZnPc in DMSO exhibited a sharp absorption band with maximum absorption at 671 nm in DMSO. Preliminary ^{1}H-NMR analysis of **BS1** in DMSO-d_6 showed four absorptions, which were due to pyridone ring protons. The two broad absorptions down filed at 8.13 and 9.20 corresponded to the two sets of phthalocyanine ring protons when compared to absorptions of an authentic sample of ZnPc in DMSO-d_6. If this **BS1** was ZnPc link pyridones, **BS1** would be expected as a regio-isomeric mixture. Thus, the triplet-like absorption at 5.75 ppm was due to absorption of the methylene protons from different regio-isomers. Based on these results, both **BS1** and **BS2** were expected as regio-isomeric mixture of Zn-phthalocyanine link pyridones **26** and phthalocyanine link pyridones **27**.

Irradiation of **BS1** in DMSO-d_6 led to consumption of all proton absorptions observed before irradiation and to formation of a new singlet at 10.22 ppm. The ^{1}H-spectrum did not show formation that would correspond to an endoperoxide. After heating, the singlet at 10.22 ppm disappeared with no recovery of pyridone protons. The blue reaction solution became dark after heating and some precipitation was observed. Irradiation of a mixture of ZnPc (catalytic amount) and N-benzyl-2-pyridone **(4)** in DMSO-d_6 was also carried out as a control experiment. The result showed consumption of the starting pyridone and formation of new products one of which corresponded to the endoperoxide **14**. After heating, the ^{1}H-spectrum showed endoperoxide consumption but no recovery of pyridone protons was observed. The blue reaction solution became dark after heating. Irradiation of mixtures of AlPc (catalytic amount) and N-benzyl-2-pyridone **(4)** in DMSO-d_6 or $CDCl_3$ were also carried out. Irradiation in DMSO-d_6 revealed similar observation to the result from the mixture containing ZnPc. Irradiation in $CDCl_3$ exhibited the formation of endoperoxide **14** which reverted back to the starting pyridone upon heating. These results lead to a preliminary conclusion that DMSO is not a suitable solvent for pyridone singlet oxygen trapping and releasing.

Covalent Attachment of Pyridones upon Porphyrin

Efforts to attach pyridones upon porphyrin **(29)** were conducted according to the synthetic route shown in Scheme 6.

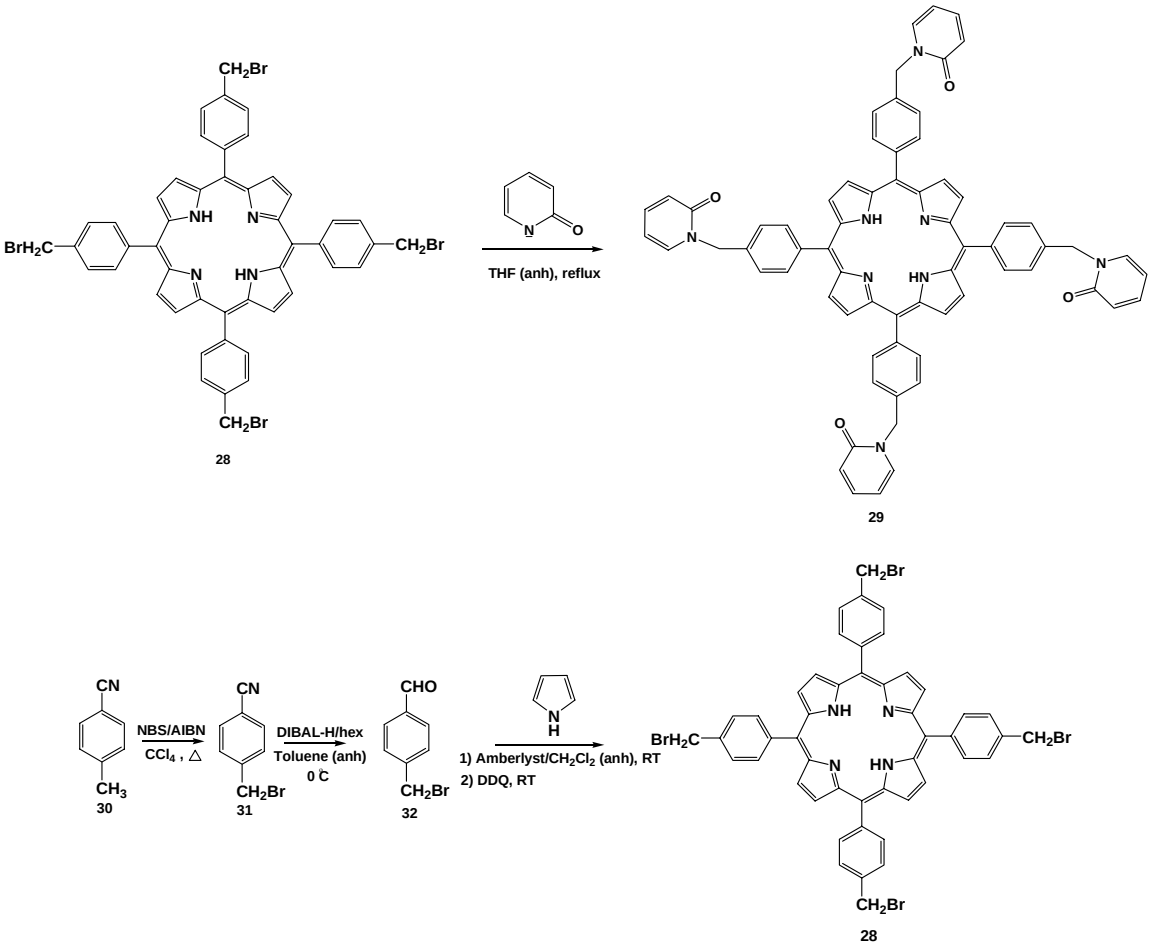

Scheme 6

Covalent linkage between pyridones and TPP via methylene bridges was confirmed by ^{1}H-NMR. In porphyrin **28**, the methylene protons appeared as a singlet at 4.85 ppm. After the coupling reaction, the ^{1}H-NMR spectrum showed a singlet downfield at 5.54 ppm and no residual singlet at 4.85 ppm was observed. The singlet at 5.54 ppm corresponded to the methylene protons bridging between pyridone rings and TPP. This indicated that the coupling occurred at all four sites of TPP.

UV-Vis absorption spectrum of porphyrin **29** in chloroform was recorded. The spectrum showed its soret-band and Q-band similar to the absorption spectrum of TPP in chloroform. The spectrum also showed a broad absorption in UV region with a maximum absorption of 296 nm. By comparison to the individual absorption spectra of TPP and N-benzyl-2-pyridone **(4)** in chloroform, the broad absorption with maximum at 296 nm corresponded to absorption of pyridone moieties. This also indicated that the UV-Vis absorption spectrum of porphyrin **29** in chloroform appeared as a combination of the TPP and N-benzyl-2-pyridone absorption spectra.

Fluorescence emission spectrum of porphyrin **29** in chloroform showed two broad emission bands with maximum emission wavelengths of 655 and 725 nm. These emission bands were consistent with the fluorescence emission spectrum of TPP in chloroform. The fluorescence excitation spectrum of

porphyrin **29** also showed a pattern similar to its absorption spectrum. Fluorescence quantum yield of porphyrin **29** in chloroform was determined relative to the known fluorescence quantum yield of TPP in chloroform of 0.11. This gave a fluorescence quantum yield for porphyrin **29** of 0.11. Fluorescence lifetime of porphyrin **29** in degassed chloroform was determined. Analysis of the fluorescence decay by single exponential function gave a lifetime of 9.66 ± 0.13 ns. Fluorescence decay of TPP in chloroform was also determined by the same instrument, which gave the TPP fluorescence lifetime of 9.93 ± 0.08 ns.

Irradiation of porphyrin **29** and TPP + pyridone **4** were carried out. All irradiations were carried out by irradiation of solutions in chloroform-d solvent employing a Xe-arc lamp through a yellow filter (λ > 500 nm) at ambient temperature. The solutions were purged with fine oxygen stream during irradiation. After each irradiation, the reaction was monitored by ^{1}H-NMR spectroscopy. The kinetics decomposition of endoperoxide moieties were carried out by recording ^{1}H-NMR spectra of the endoperoxide consumption from porphyrin **33** in chloroform-d solvent as a function of time at various temperatures.

After irradiation of porphyrin **29** solution for 20 min, the ^{1}H-NMR overlay spectra (Figure 1) indicated approximately 90 % consumption of the pyridone moieties (*) and also demonstrated formation of new proton signals as labeled *. These new proton absorptions were consistent with the formation of the corresponding endoperoxide moieties **(33)** from oxidation of pyridone moieties by singlet oxygen compared to the known result from the control experiment (Figure 2). After heating the irradiated solution at 40 °C for 30 min, Figure 1 showed the consumption of the endoperoxide moieties and recovery of pyridone moieties. This experiment was repeated for three cycles. The overlay spectra exhibited reversible trapping and releasing of singlet oxygen throughout these cycles without detectable decomposition or side reactions.

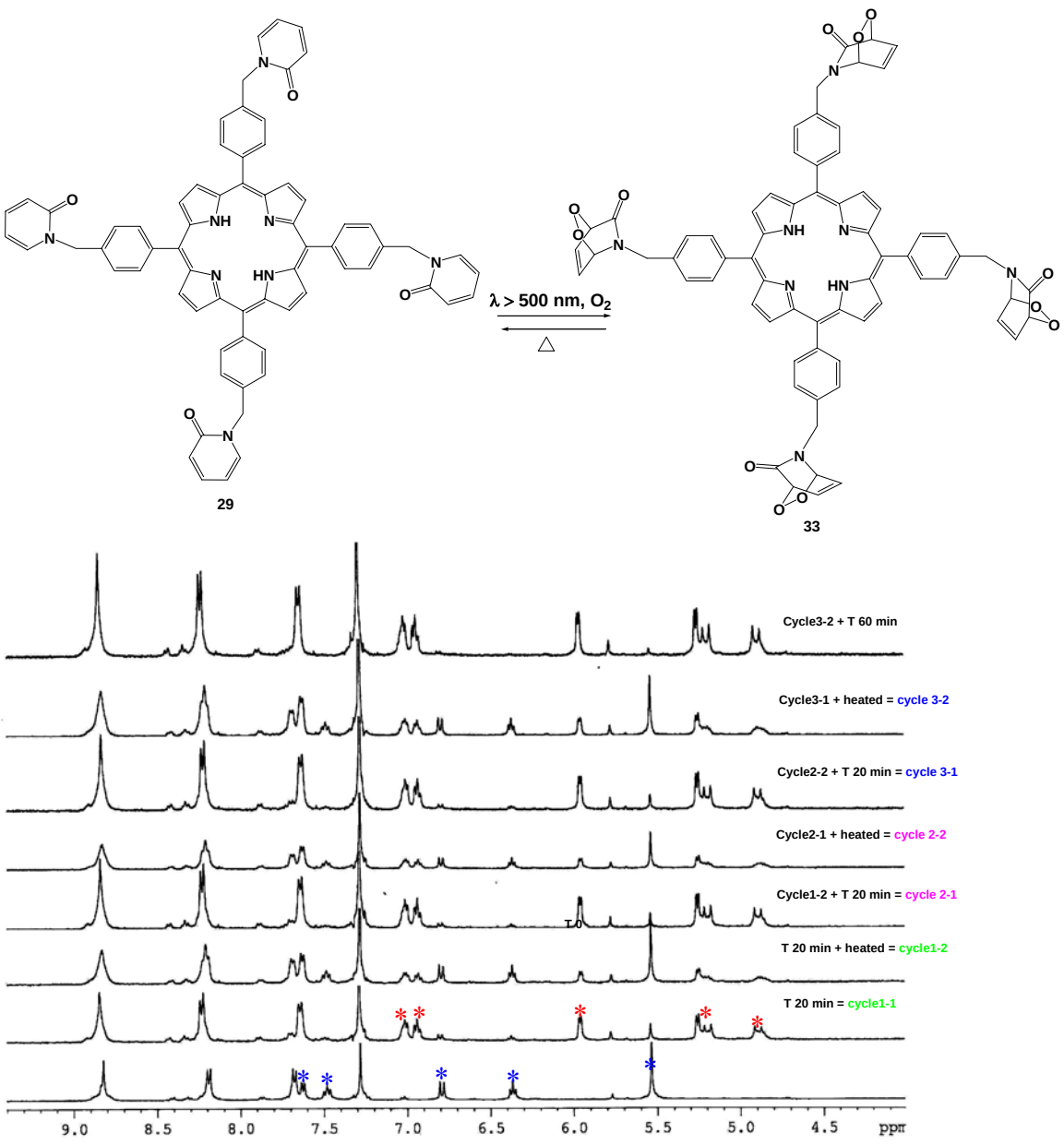
λ > 500 nm, O2
29
33
Cycle3-2 + T 60 min
Cycle3-1 + heated = cycle 3-2
Cycle2-2 + T 20 min = cycle 3-1
Cycle2-1 + heated = cycle 2-2
Cycle1-2 + T 20 min = cycle 2-1
T 0
T 20 min + heated = cycle1-2
T 20 min = cycle1-1
9.0
8.5
8.0
7.5
7.0
6.5
6.0
5.5
5.0
4.5
ppm

Figure 1

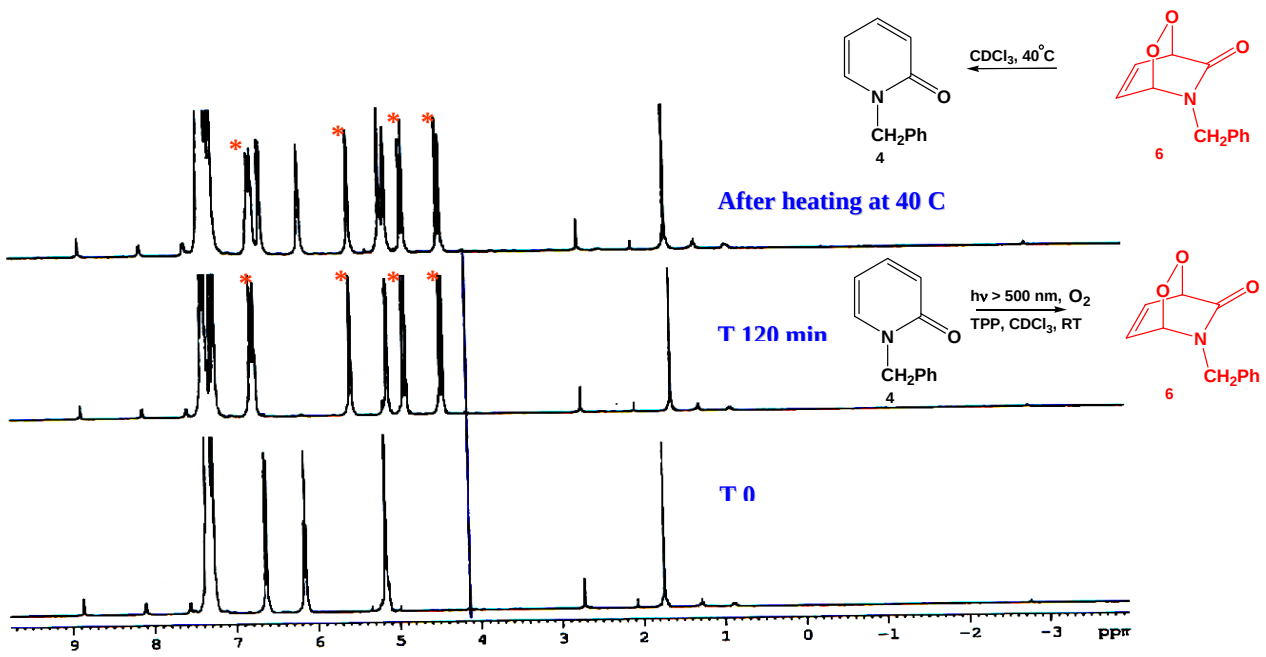

Figure 2

Figure 3 shows plots of ln[endo] Vs time at various temperatures. These plots indicate that the decomposition of endoperoxides link porphyrin is a first order reaction similar to the results observed in the corresponding unlinked endoperoxide complex.

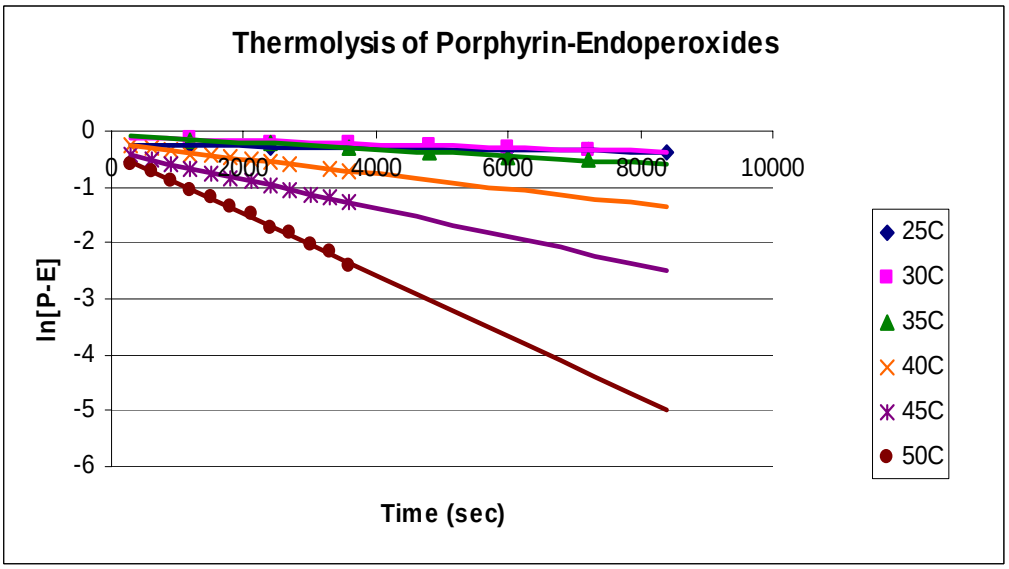

Figure 3

Figure 4 shows plot between 1/T Vs ln(k/T). From this plot, thermodynamics parameters at 298 K can be determined; $\Delta H^{\neq}$ = 26.73±0.47 kcal/mol, $\Delta S^{\neq}$ = 9.05±1.50 cal/mol, $\Delta G^{\neq}$ = 24.03±0.02 kcal/mol.

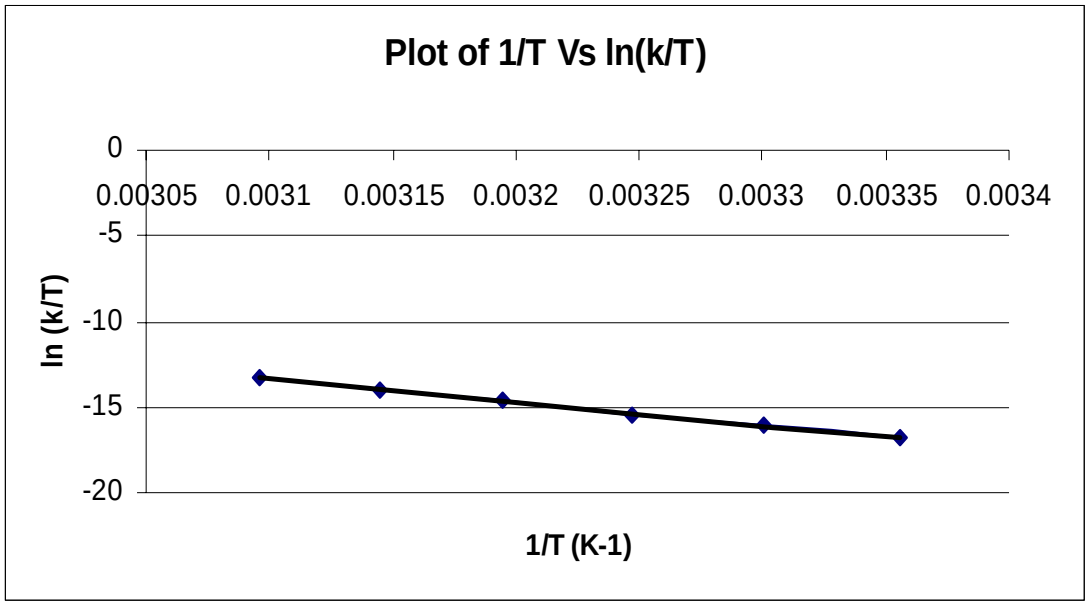

Spectroscopic results of porphyrin **29** revealed that attachment of pyridones to TPP via methylene bridges did not adversely perturb the excited state of TPP. Kinetics studies reveale that covalent linkage of pyridones upon porphyrin photosensitizer exhibited decomposition / singlet oxygen release kinetics similar to those observed for unmodified pyridones.